Geoscientific
Model Development

Open Access

Discussions

Supplement of

ECCO version 4: an integrated framework for non-linear inverse modeling and global ocean state estimation

G. Forget et al.

Correspondence to: G. Forget (gforget@mit.edu)

standard analysis of ECCO-Production, release 1 state estimate (the baseline ECCO version 4 solution)

February 20, 2015

Table of contents

ECCO v4 ocean state estimate, release 1
estimate source : Gael Forget, MIT/AER/JPL ECCO-Production group
support contact : ecco-support@mit.edu
internal code : r4it11
estimate revision history :
r4it11 : reduce background vertical viscosity
r4it10 : cleanup control vector adjustments
r4it9 : optim. global mean sea level alone
r4it0-8 : full adjoint iterations, omitting
global mean sea level altimetry constraint.
files revision history :
2014/02/04 : initial release of ECCO v4 (GF)
- domain decomposed in 90x90 tiles (13 of them)
- CF-1.6 ncetcdf files (using write
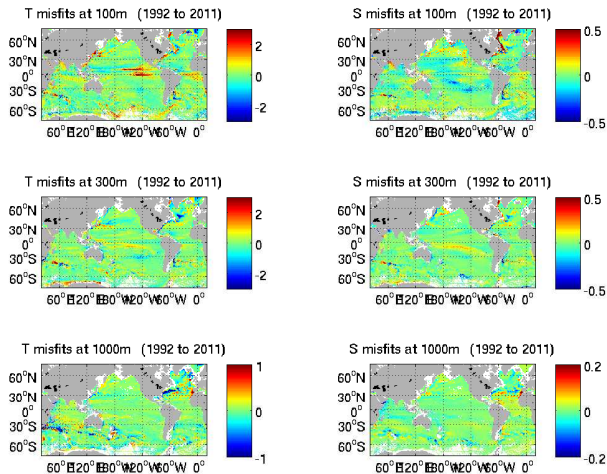
fit to in situ data

Figure: Time mean misfit (model-data) for in situ profiles, at various depths (rows), for T (left; in K) and S (right; in psu).
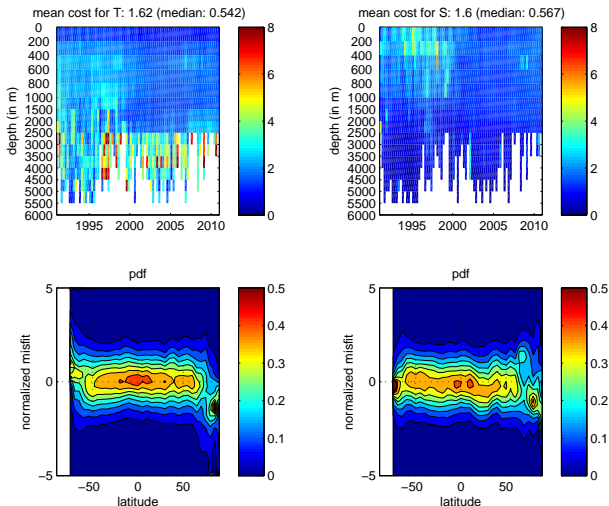
fit to in situ data

Figure: Cost function (top) for in situ profiles, as a function of depth and time. Distribution of normalized misfits (bottom) as a function of latitude. For T (left) and S (right).
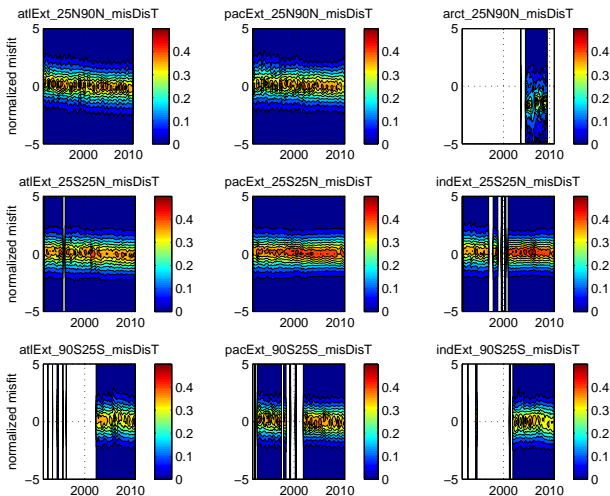
fit to in situ data

Figure: Distribution of normalized misfits per basin (panel) as a function of latitude, for T
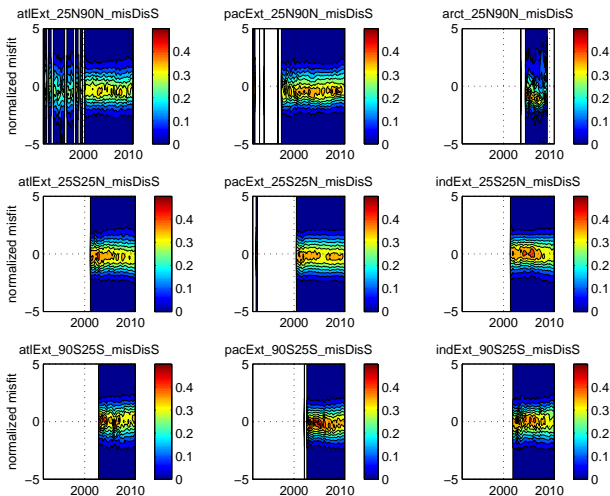
fit to in situ data

Figure: Distribution of normalized misfits per basin (panel) as a function of latitude, for S
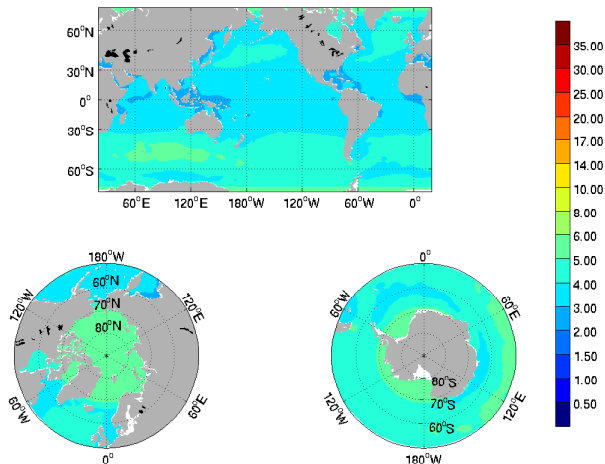
fit to altimeter data (RADS)

Figure: mean dynamic topography prior uncertainty (cm)
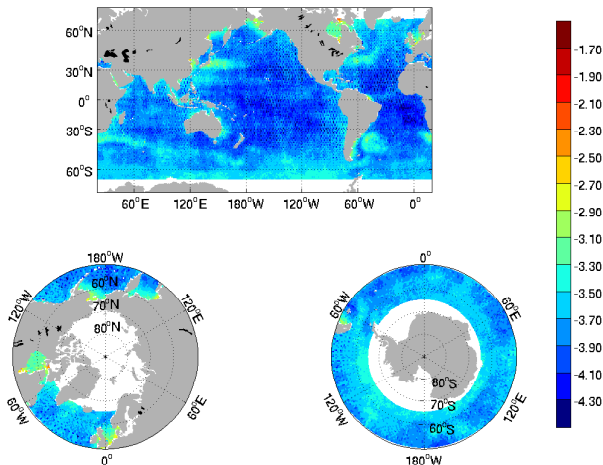
fit to altimeter data (RADS)

Figure: log(prior error variance) – sea level anomaly (m^2) – large space/time scales
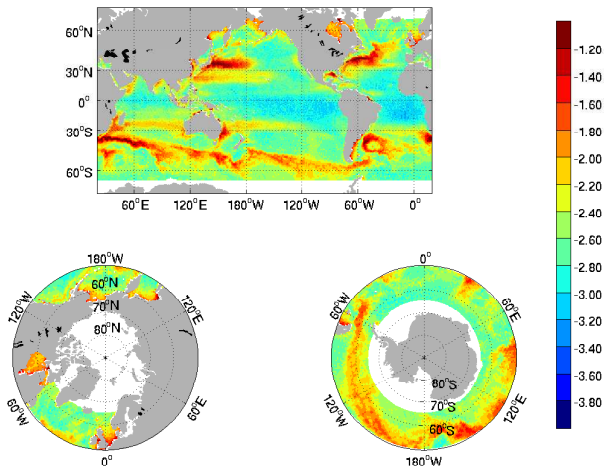
fit to altimeter data (RADS)

Figure: log(prior error variance) – sea level anomaly (m^2) – pointwise
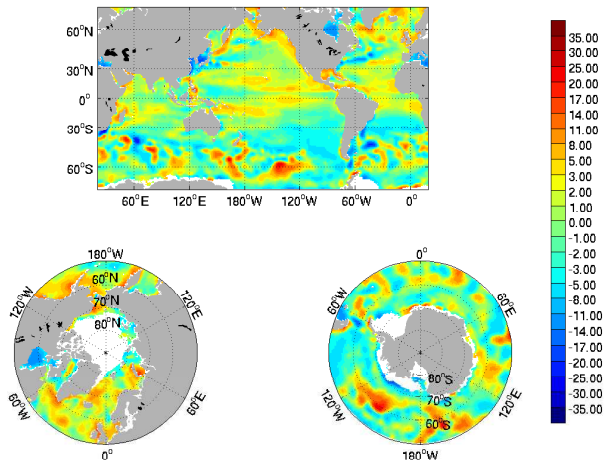
fit to altimeter data (RADS)

Figure: mean dynamic topography misfit (cm)
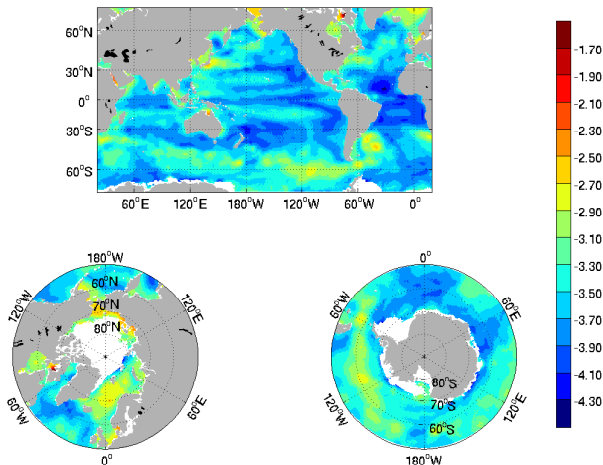
fit to altimeter data (RADS)

Figure: modeled-observed log(variance) – sea level anomaly (m^2) –
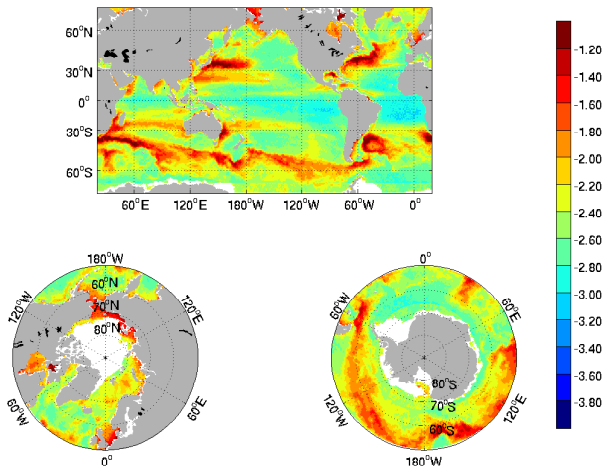large space/time scales

fit to altimeter data (RADS)

Figure: modeled-observed log(variance) – sea level anomaly (m^2) – pointwise

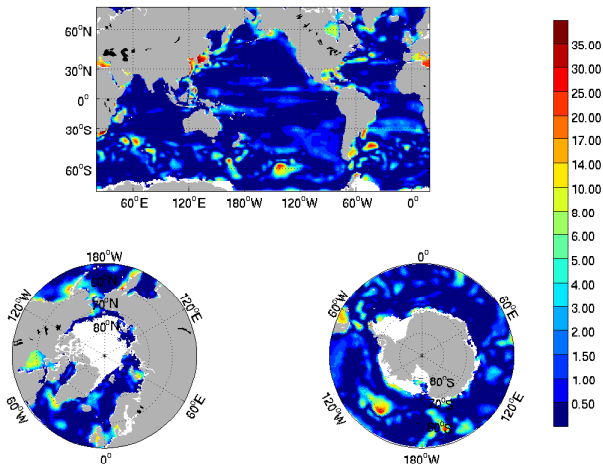# fit to altimeter data (RADS)

Figure: modeled-observed cost – mean dynamic topography
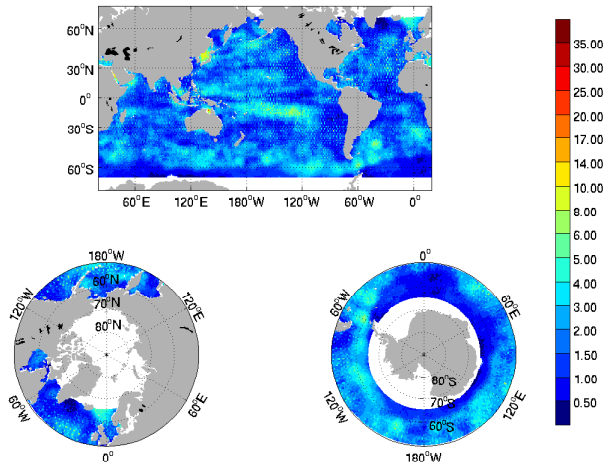
fit to altimeter data (RADS)

Figure: modeled-observed cost – sea level anomaly
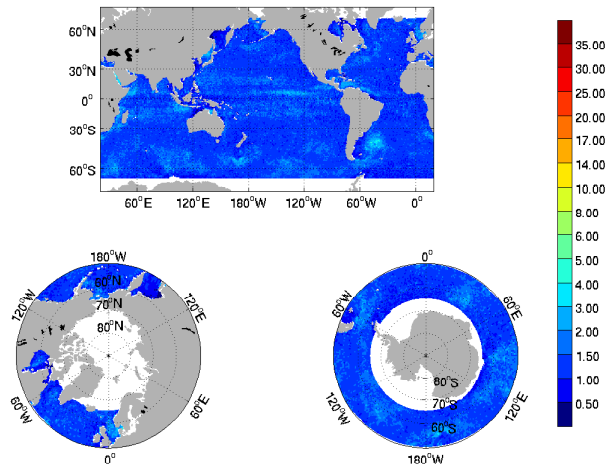– large space/time scales

fit to altimeter data (RADS)

Figure: modeled-observed cost – sea level anomaly – pointwise
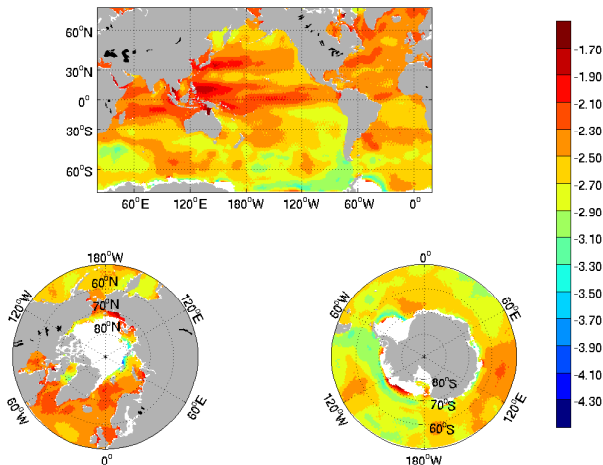
fit to altimeter data (RADS)

Figure: observed log(variance) – sea level anomaly (m^2) – large space/time scales
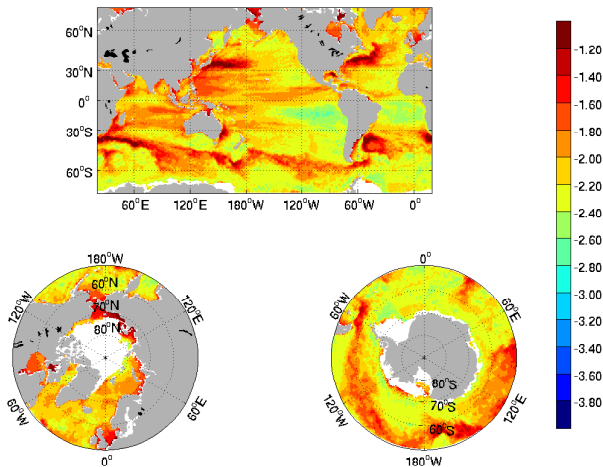
fit to altimeter data (RADS)

Figure: observed log(variance) – sea level anomaly (m^2) – pointwise
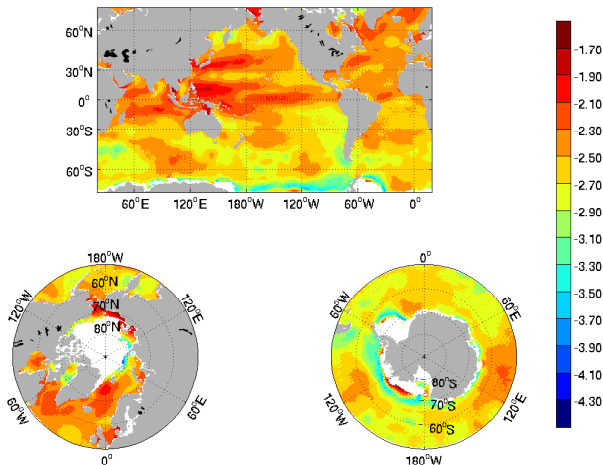
fit to altimeter data (RADS)

Figure: modeled log(variance) – sea level anomaly (m^2) – large space/time scales

fit to altimeter data (RADS)
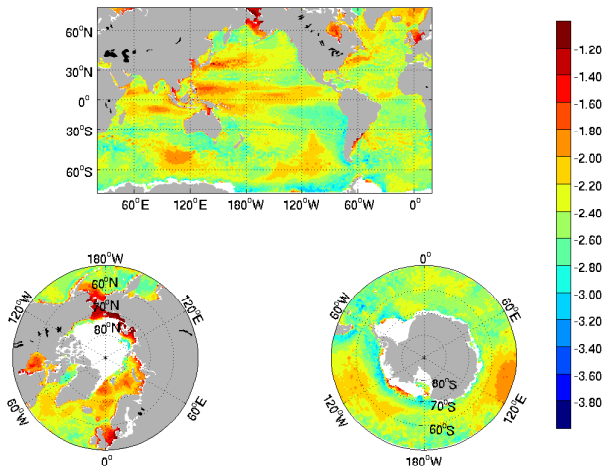

Figure: modeled log(variance) – sea level anomaly (m^2) – pointwise
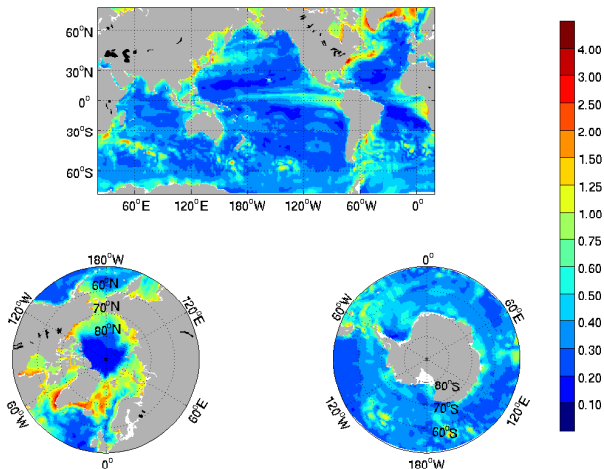
fit to sst data

Figure: modeled-Reynolds rms – sea surface temperature (K)
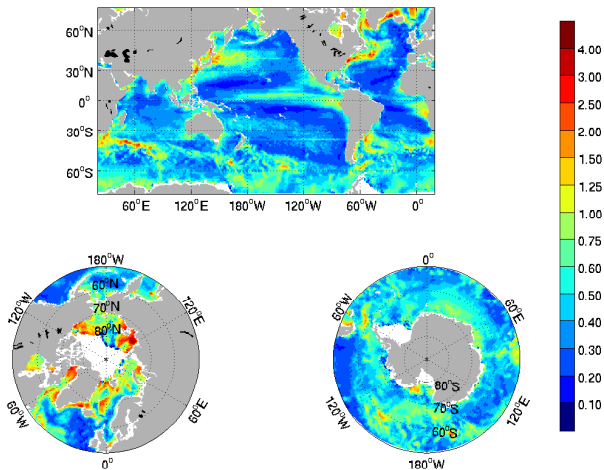
fit to sst data

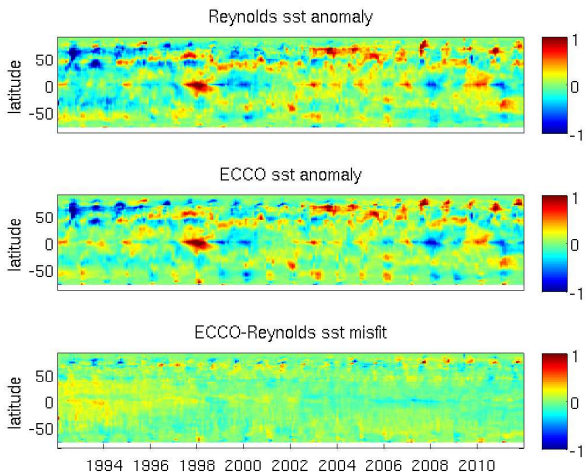Figure: modeled-REMSS rms – sea surface temperature (K)

fit to sst data

Figure: ECCO and Reynolds zonal mean sst anomalies (K)
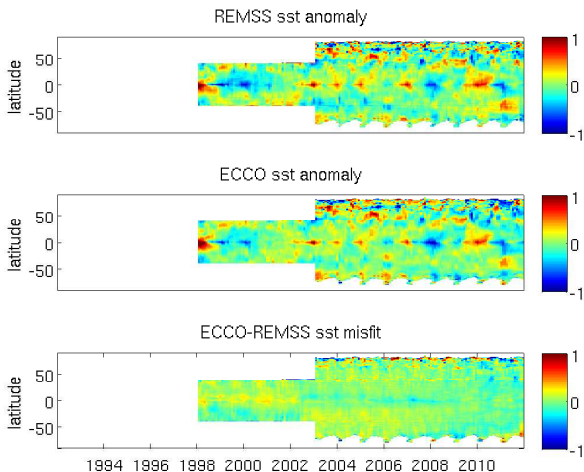
fit to sst data

Figure: ECCO and REMSS zonal mean sst anomalies (K)
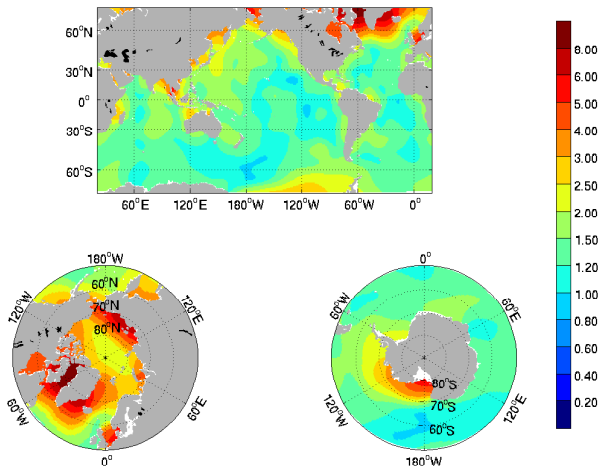
fit to grace r4 data

Figure: modeled-observed rms – bottom pressure (cm)

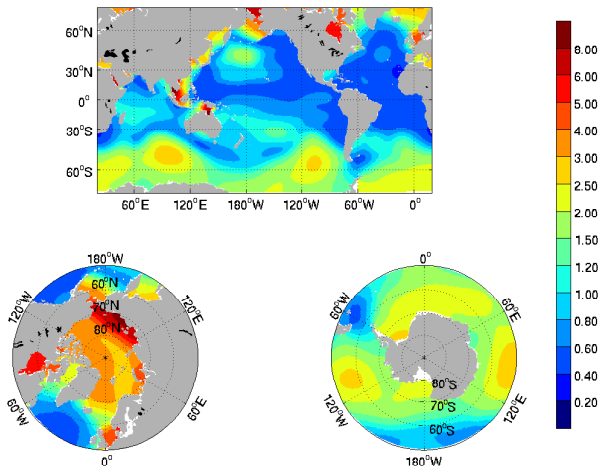# fit to grace r4 data

Figure: rms modeled – bottom pressure (cm)
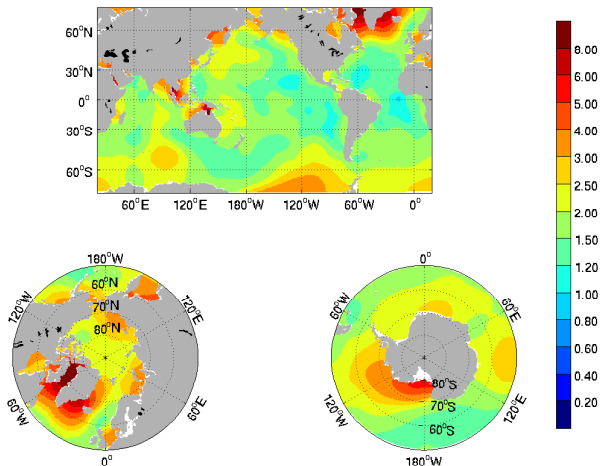
fit to grace r4 data

Figure: rms observed – bottom pressure (cm)
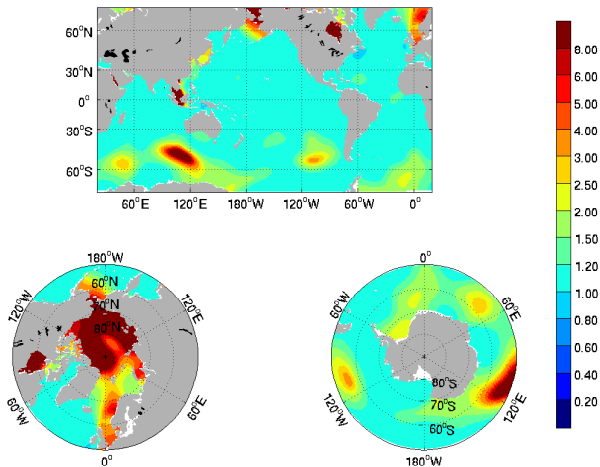
fit to grace r4 data

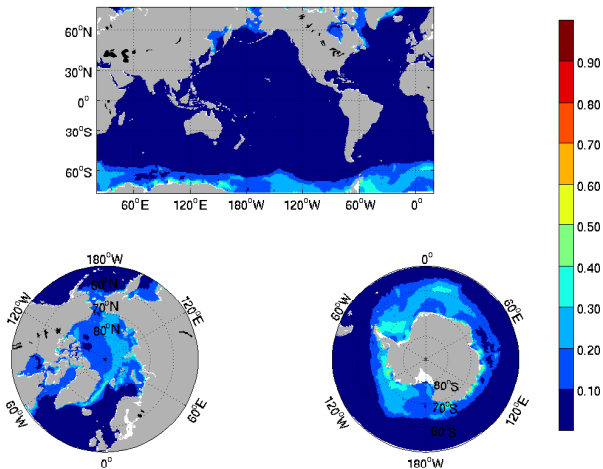Figure: Cost function

fit to seaice data

Figure: modeled-observed rms – sea ice concentration
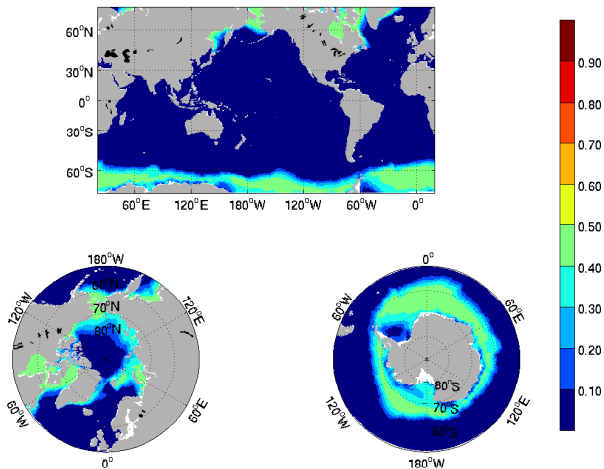
fit to seaice data

Figure: observed std – sea ice concentration
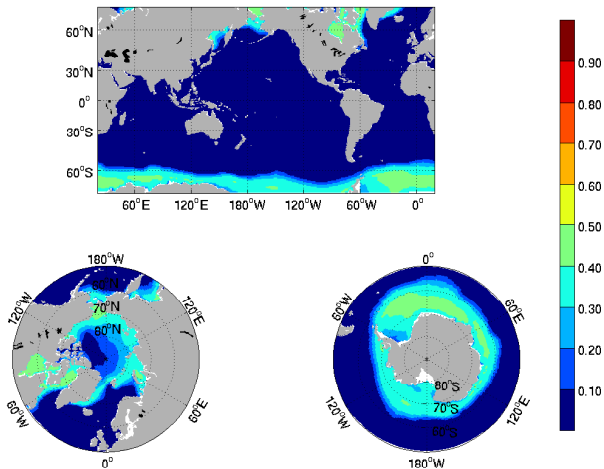
fit to seaice data

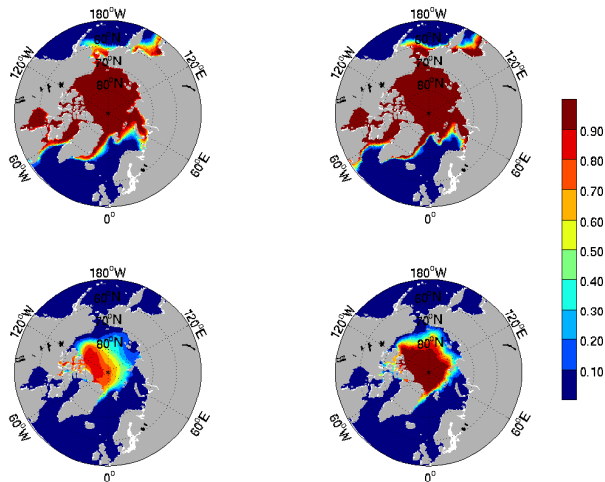Figure: modelled std – sea ice concentration

fit to seaice data

Figure: ECCO (left) and NSIDC (right, gsfc bootstrap) ice concentration in March (top) and September (bottom).
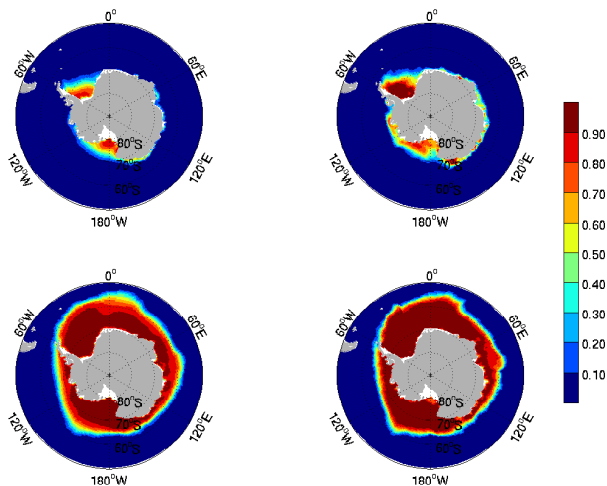
fit to seaice data

Figure: ECCO (left) and NSIDC (right, gsfc bootstrap) ice concentration in March (top) and September (bottom).
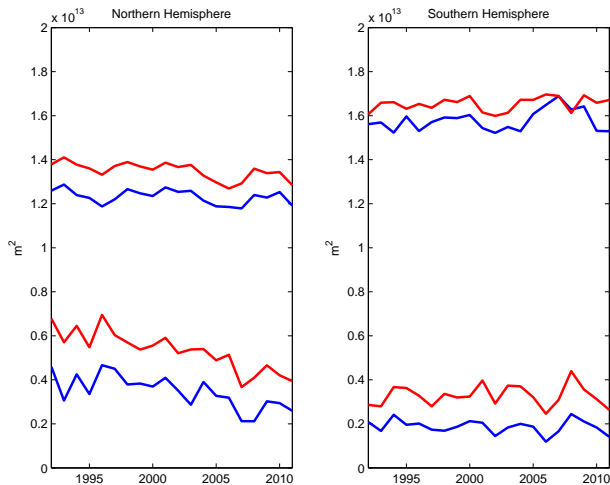
fit to seaice data

Figure: ECCO (blue) and NSIDC (red, gsfc bootstrap) ice concentration in March and September in Northern Hemisphere (left) and Southern Hemisphere (right)
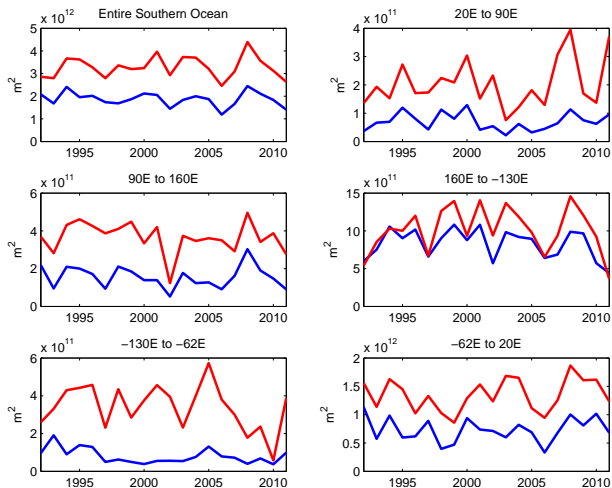
fit to seaice data

Figure: ECCO (blue) and NSIDC (red, gsfc bootstrap) ice
concentration in March per Southern Ocean sector
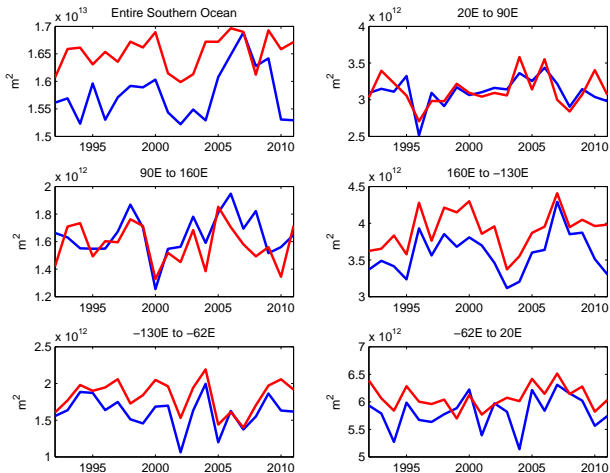
fit to seaice data

Figure: ECCO (blue) and NSIDC (red, gsfc bootstrap) ice concentration in September per Southern Ocean sector
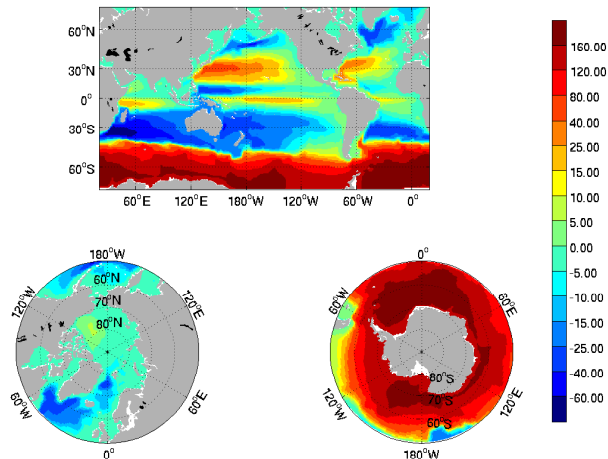
barotropic streamfunction

Figure: 1992-2011 mean – barotropic streamfunction (Sv)
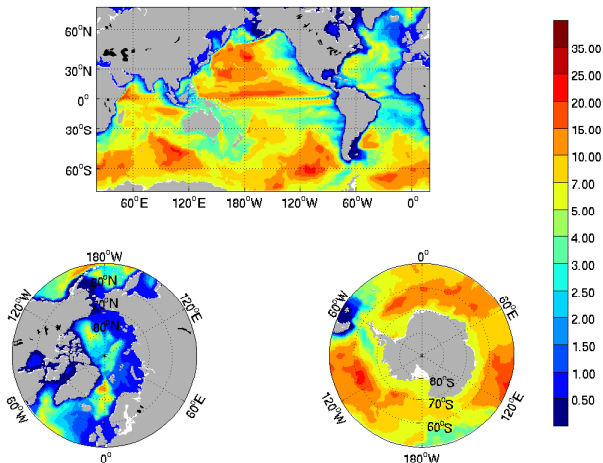
barotropic streamfunction

Figure: 1992-2011 standard deviation – barotropic streamfunction (Sv)
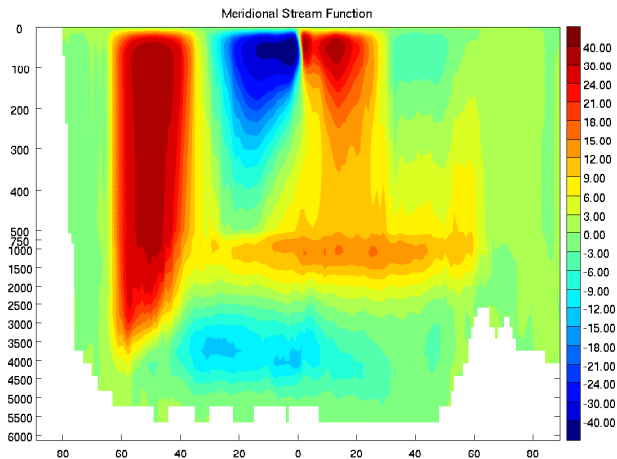
meridional streamfunction

Figure: 1992-2011 mean – overturning streamfunction (Sv)
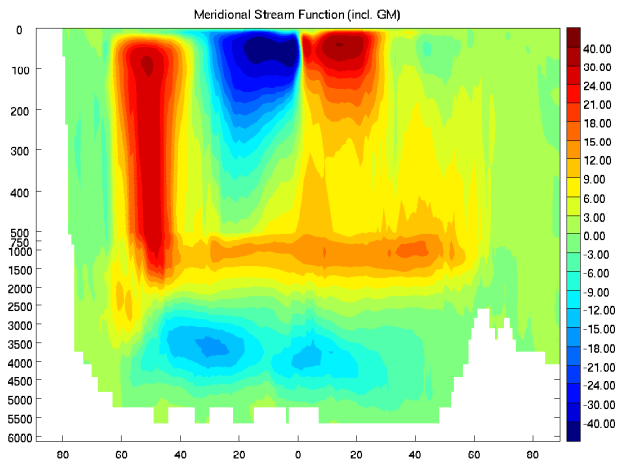
meridional streamfunction

Figure: 1992-2011 mean – overturning streamfunction incl. GM (Sv)
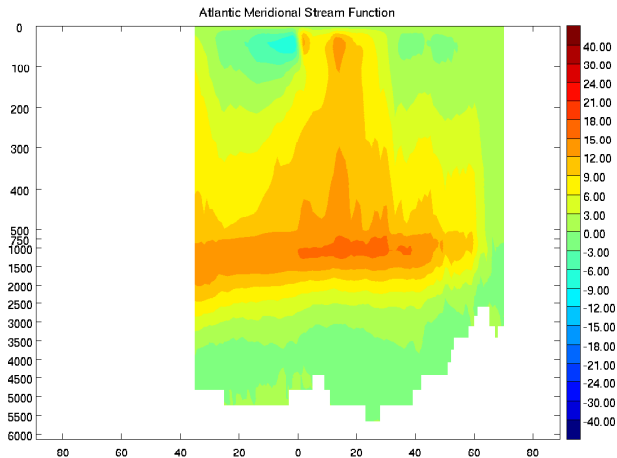
meridional streamfunction

Figure: 1992-2011 mean – Atlantic overturning streamfunction (Sv)

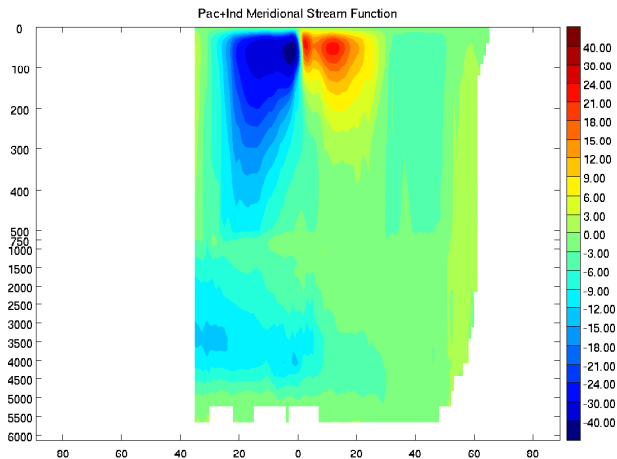# meridional streamfunction

Figure: 1992-2011 mean – Pac+Ind overturning streamfunction (Sv)
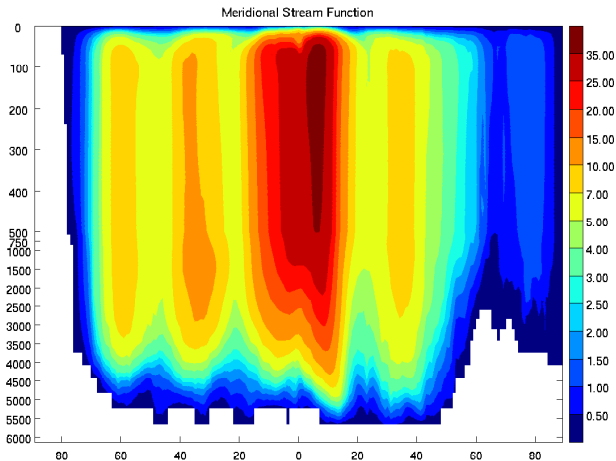
meridional streamfunction

Figure: 1992-2011 standard deviation – overturning streamfunction (Sv)
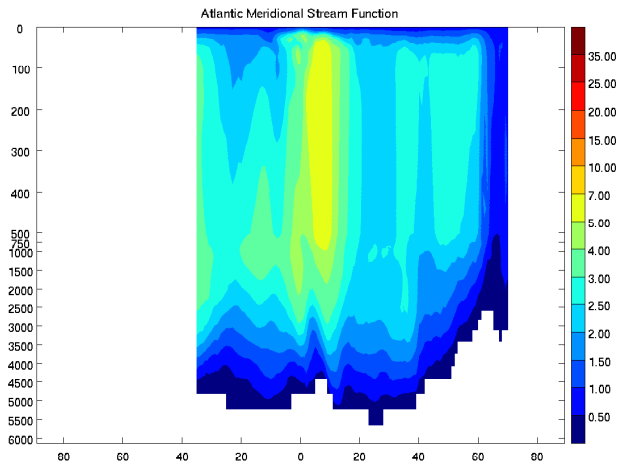
meridional streamfunction

Figure: 1992-2011 standard deviation – Atlantic overturning streamfunction (Sv)
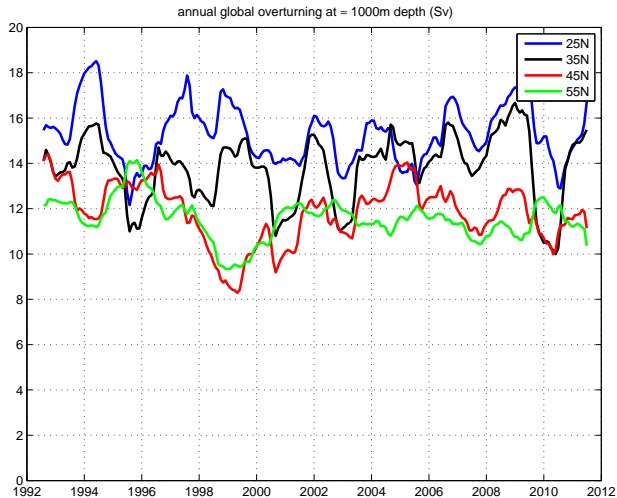
meridional streamfunction (time series)

annual global overturning at ≈ 1000m depth (Sv)

Figure: annual global overturning at select latitudes at $\approx$ 1000m depth
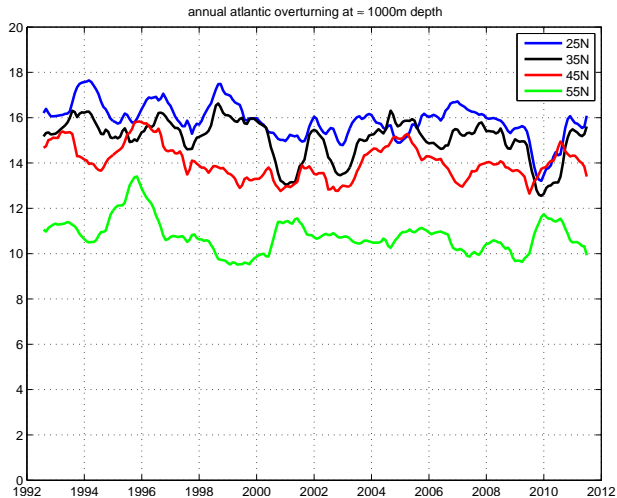
meridional streamfunction (time series)

Figure: annual Atlantic overturning at select latitudes at $\approx$ 1000m depth (Sv)
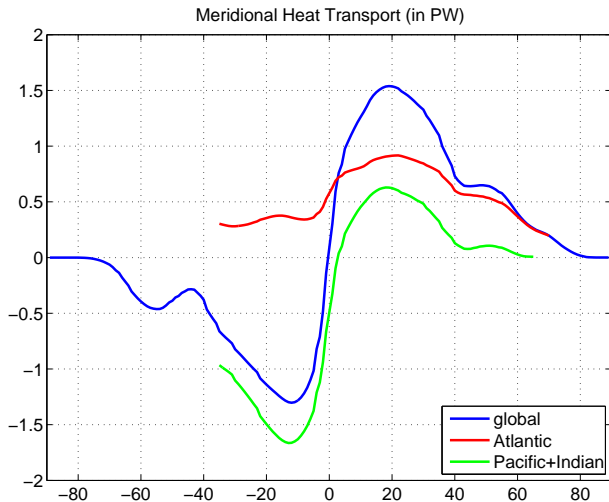
meridional heat transport

Figure: 1992-2011 mean – meridional heat transport (PW)
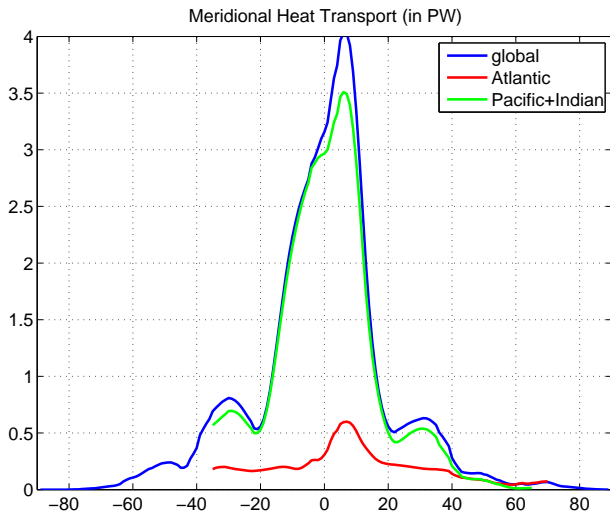
meridional heat transport

Figure: 1992-2011 standard deviation – meridional heat transport (PW)
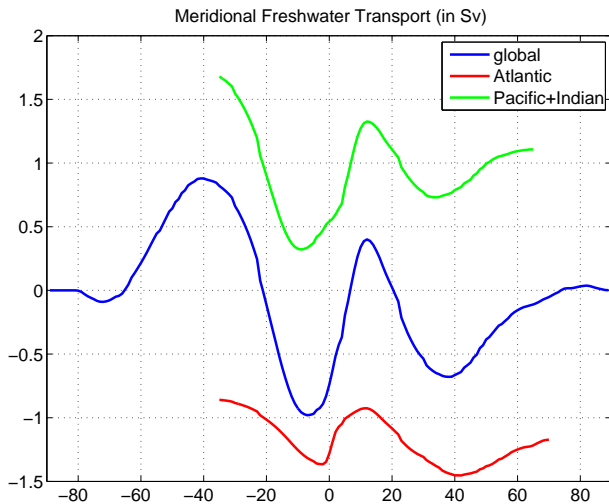
meridional freshwater transport

Figure: 1992-2011 mean – meridional freshwater transport (Sv)
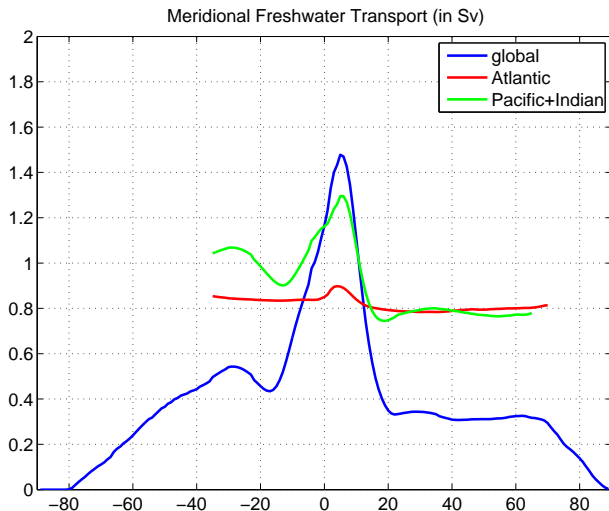
meridional freshwater transport

Figure: 1992-2011 standard deviation – meridional freshwater transport (Sv)
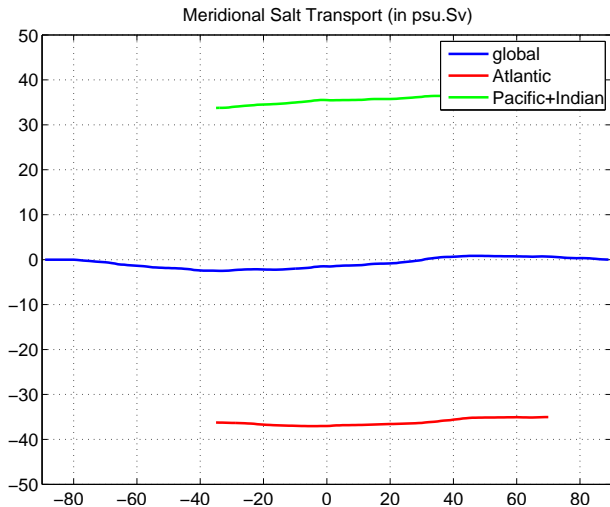
meridional salt transport

Figure: 1992-2011 mean – meridional salt transport (psu.Sv)
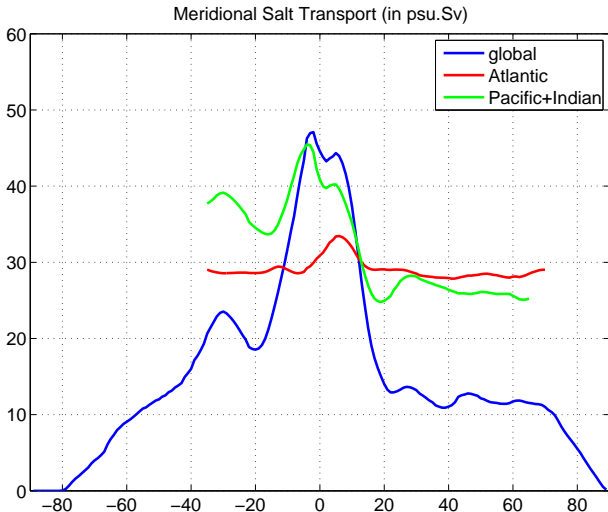
meridional salt transport

Figure: 1992-2011 standard deviation – meridional salt transport (psu.Sv)
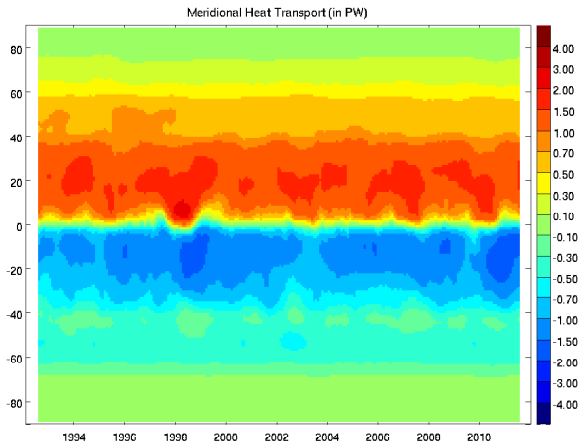
meridional transports (time series)

Figure: meridional heat transport (PW, annual mean)

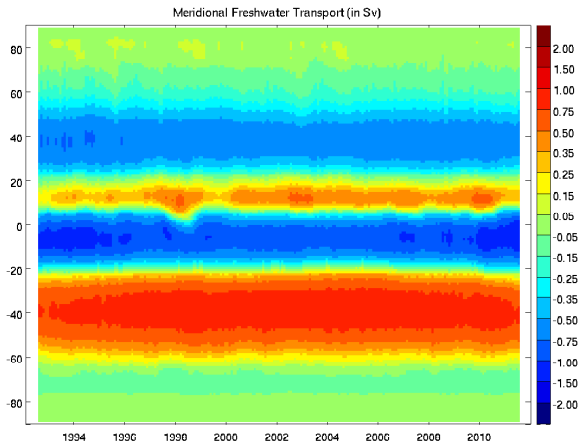# meridional transports (time series)

Figure: meridional freshwater transport (Sv, annual mean)
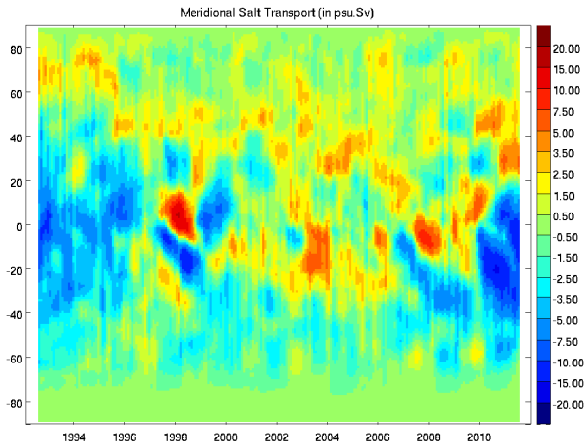
meridional transports (time series)

Figure: meridional salt transport (psu.Sv, annual mean)
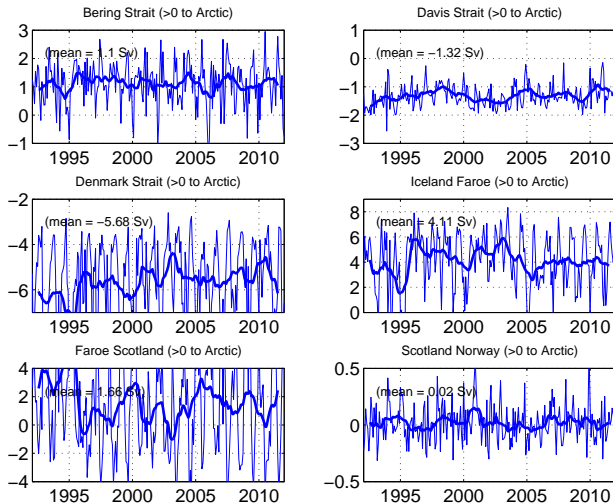
transects transport

Figure: volume transports entering the Arctic (Sv, annual mean)
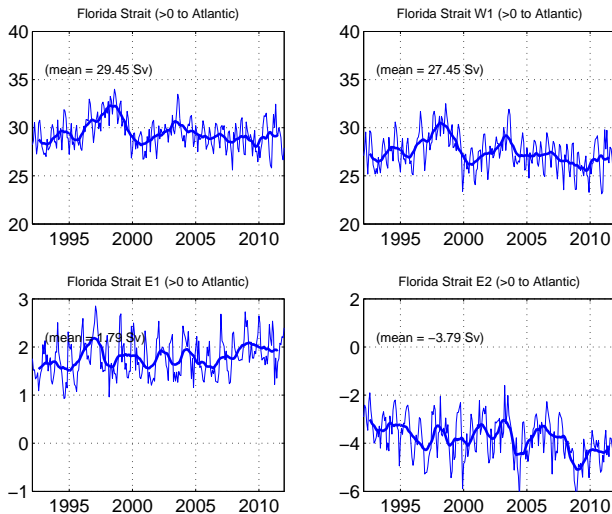
transects transport

Figure: volume transports entering the Atlantic (Sv, annual mean)
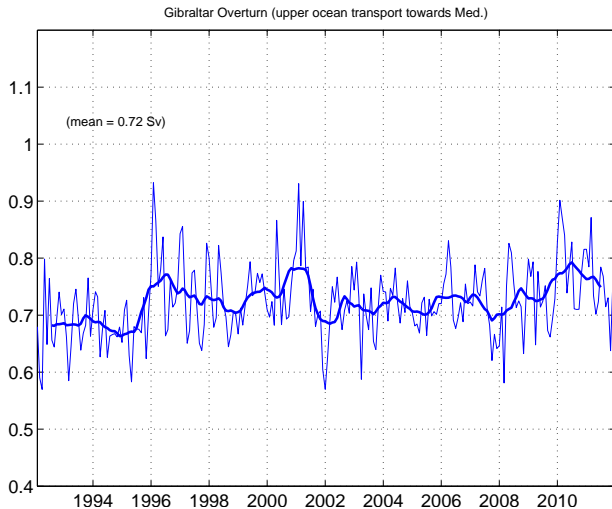
transects transport

Figure: Gibraltar Overturn (Sv, annual mean)
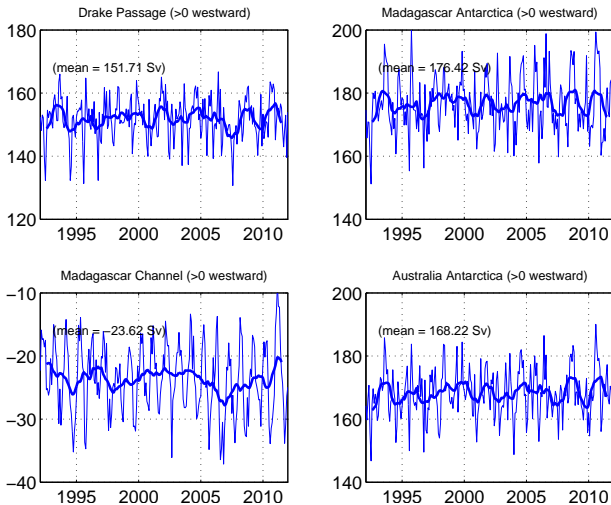
transects transport

Figure: ACC volume transports (Sv, annual mean)
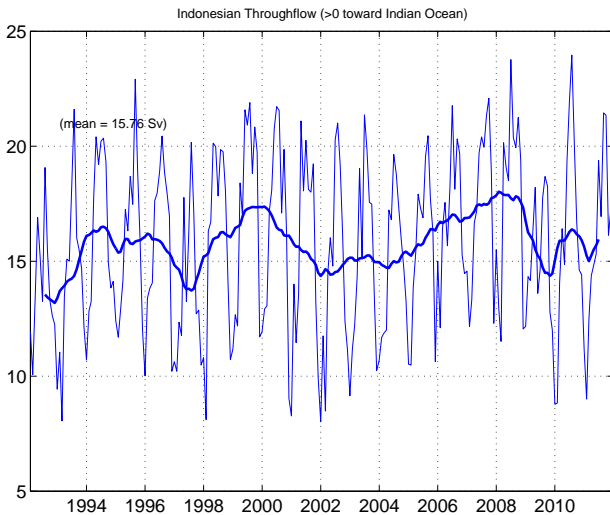
transects transport

Figure: Indonesian Throughflow (Sv, annual mean)
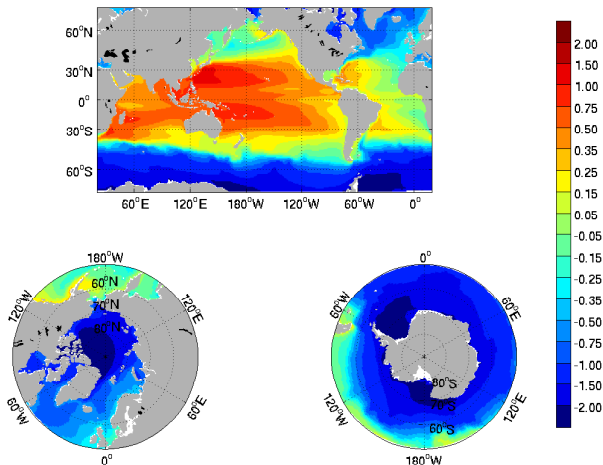
sea surface height

Figure: 1992-2011 mean – sea surface height (EXCLUDING ice, in m)
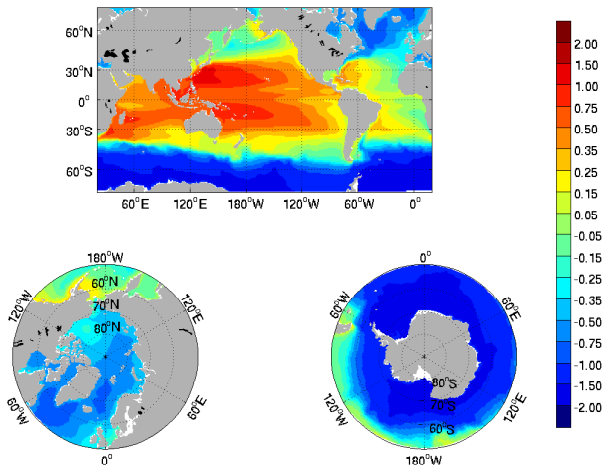
sea surface height

Figure: 1992-2011 mean – sea surface height (INCLUDING ice, in m)
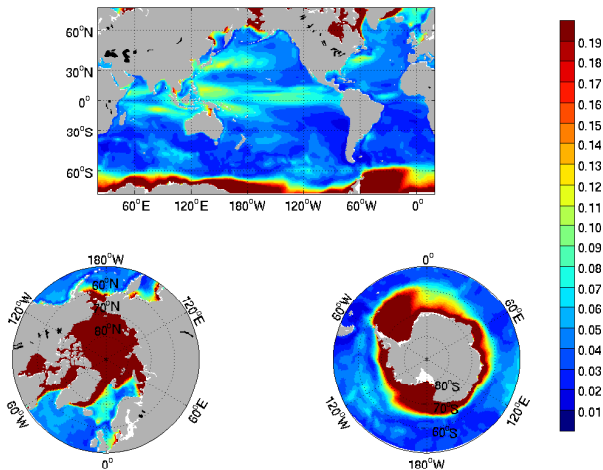
sea surface height

Figure: 1992-2011 standard deviation – sea surface height (EXCLUDING ice, in m)
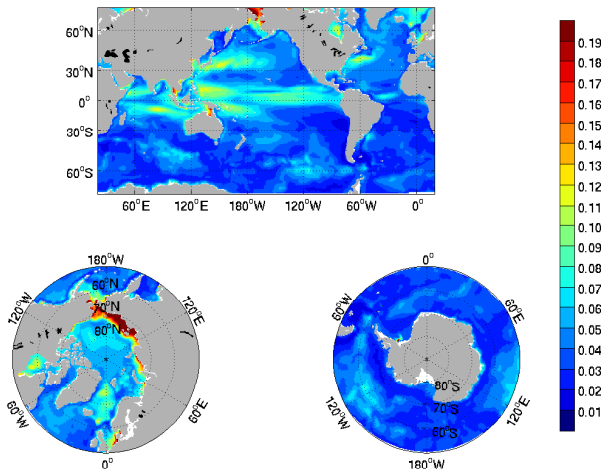
sea surface height

Figure: 1992-2011 standard deviation – sea surface height (INCLUDING ice, in m)
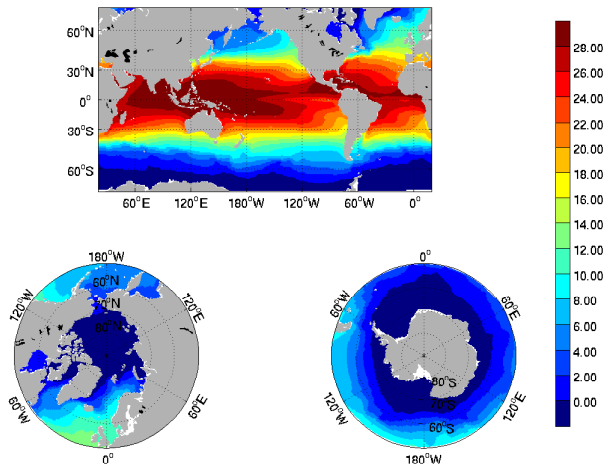
3D state variables

Figure: 1992-2011 mean – temperature (in degC) at 5m
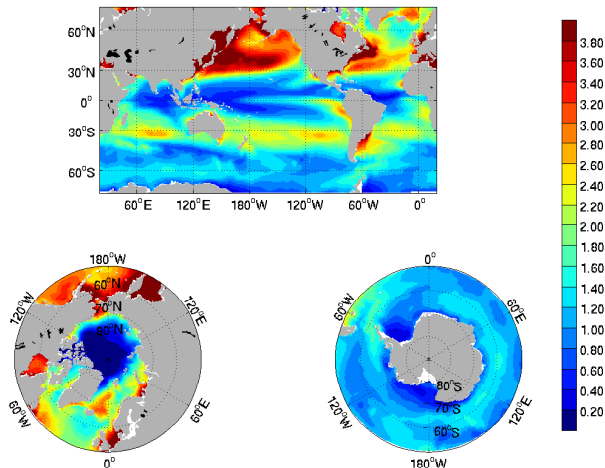
3D state variables

Figure: 1992-2011 standard deviation – temperature (in degC) at 5m

3D state variables
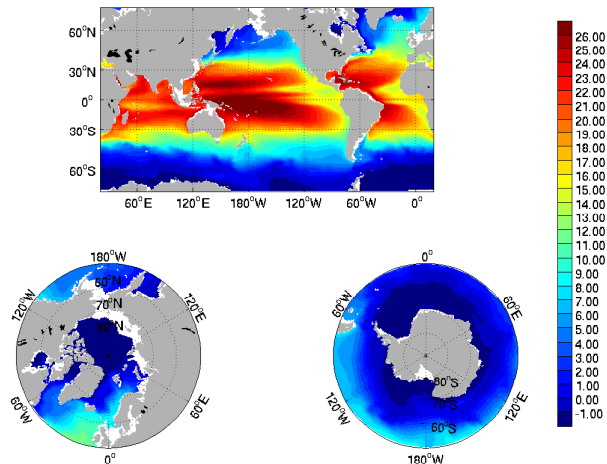

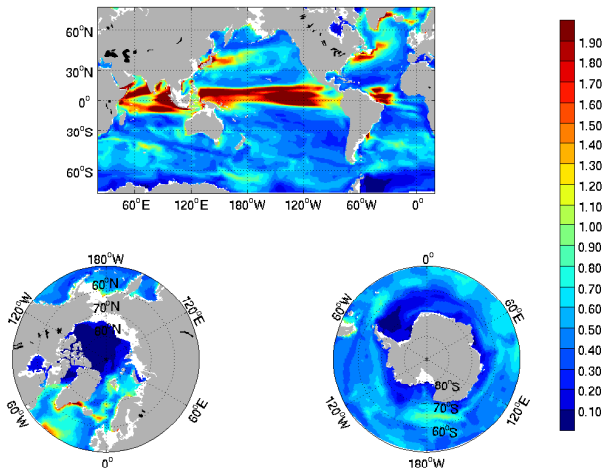Figure: 1992-2011 mean – temperature (in degC) at 105m

3D state variables

Figure: 1992-2011 standard deviation – temperature (in degC) at 105m
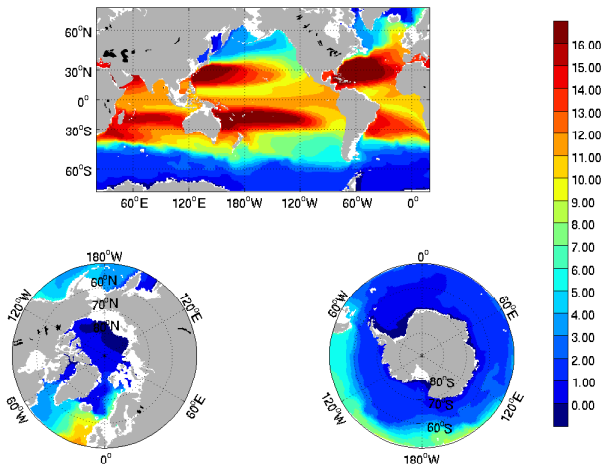
3D state variables

Figure: 1992-2011 mean – temperature (in degC) at 300m
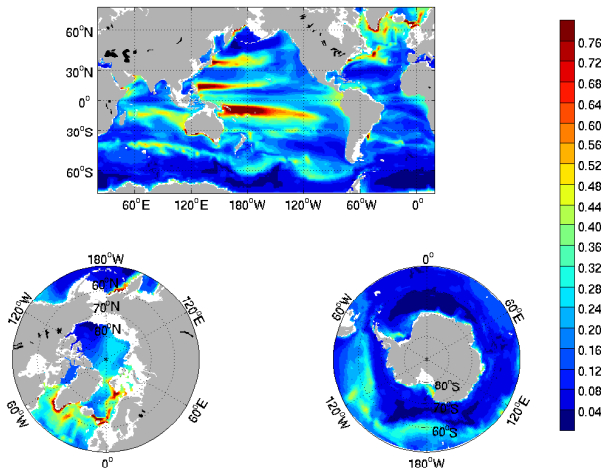
3D state variables

Figure: 1992-2011 standard deviation – temperature (in degC) at 300m
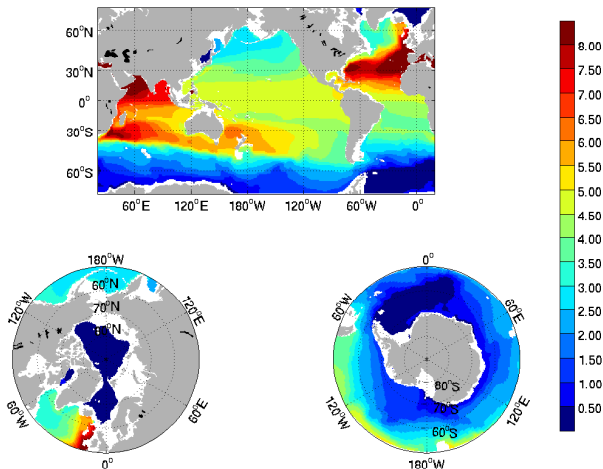
3D state variables

Figure: 1992-2011 mean – temperature (in degC) at 910m
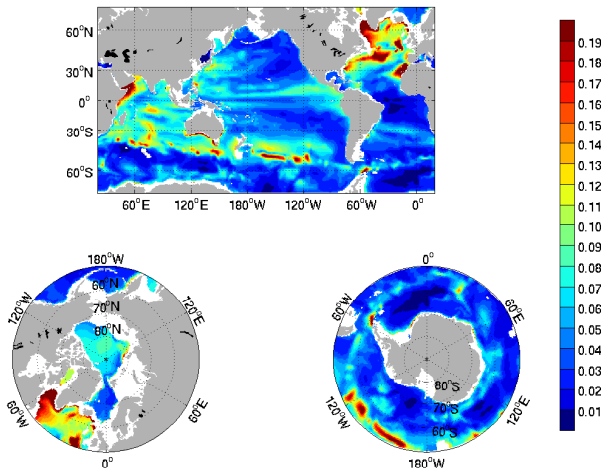
3D state variables

Figure: 1992-2011 standard deviation – temperature (in degC) at 910m

3D state variables
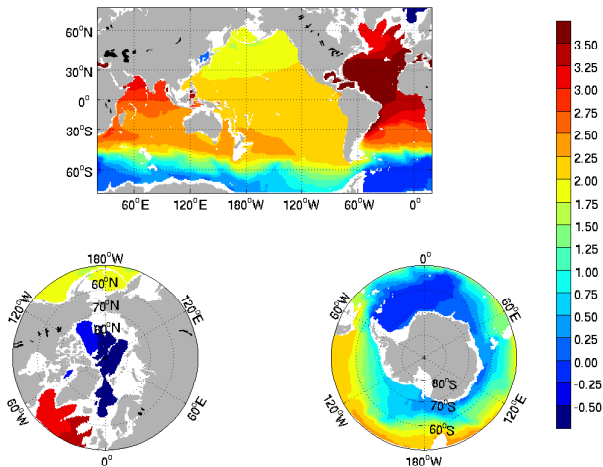

Figure: 1992-2011 mean – temperature (in degC) at 1914m

3D state variables
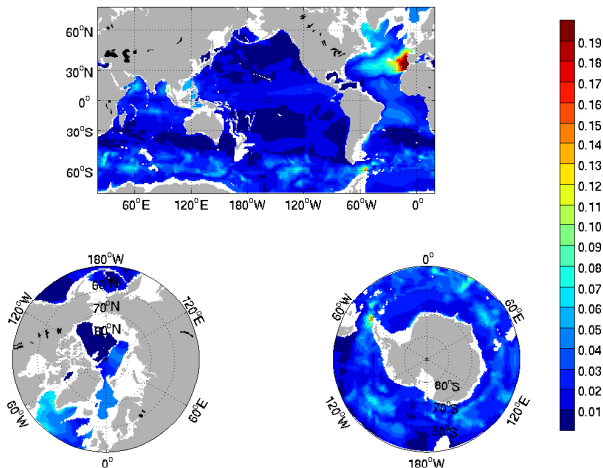

Figure: 1992-2011 standard deviation – temperature (in degC) at 1914m

3D state variables
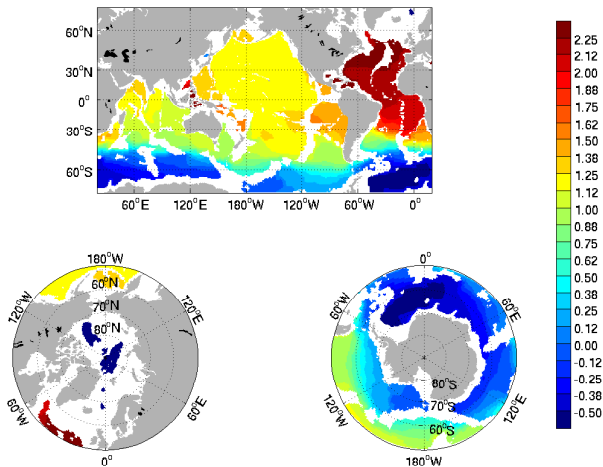

Figure: 1992-2011 mean – temperature (in degC) at 3581m
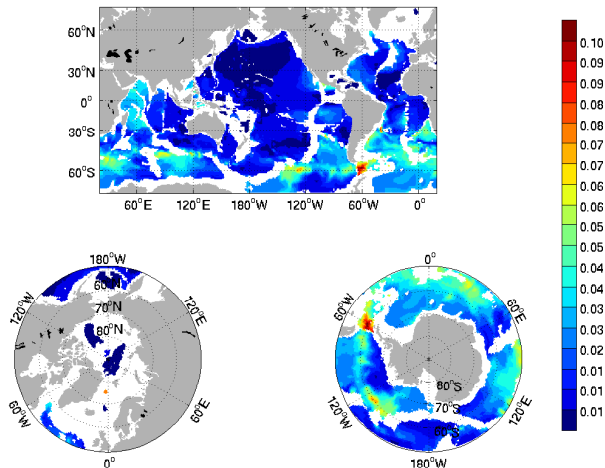
3D state variables

Figure: 1992-2011 standard deviation – temperature (in degC) at 3581m
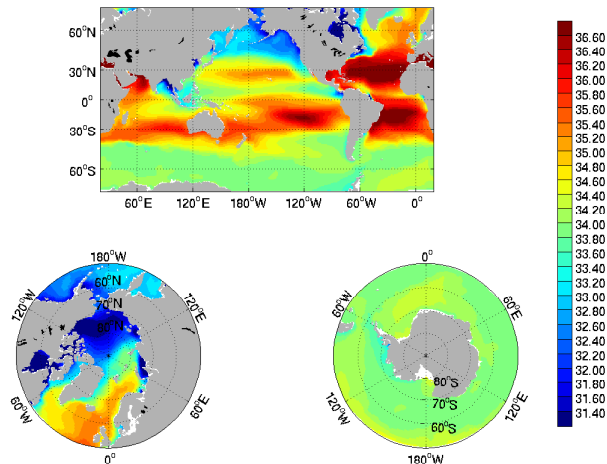
3D state variables

Figure: 1992-2011 mean – salinity (in psu) at 5m
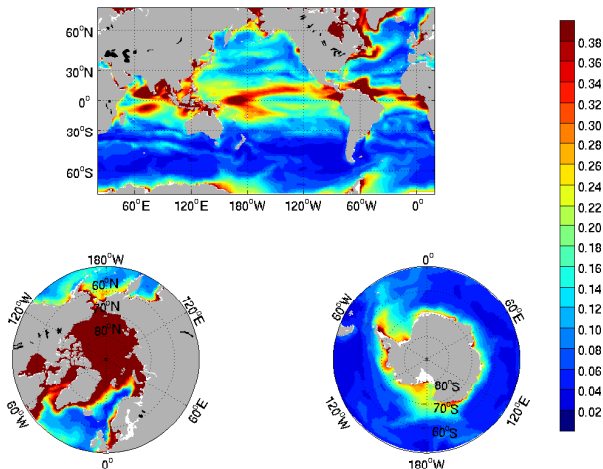
3D state variables

Figure: 1992-2011 standard deviation – salinity (in psu) at 5m
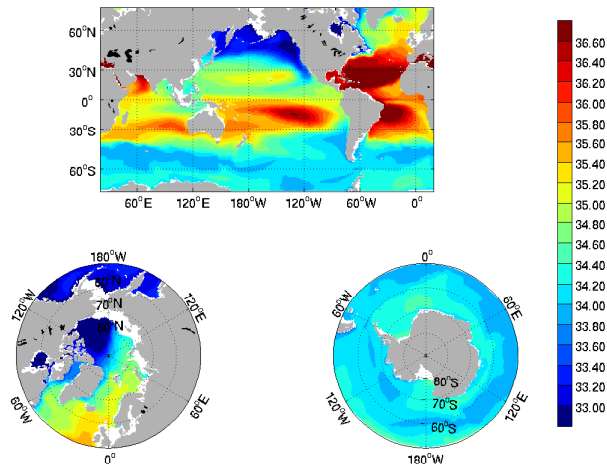
3D state variables

Figure: 1992-2011 mean – salinity (in psu) at 105m
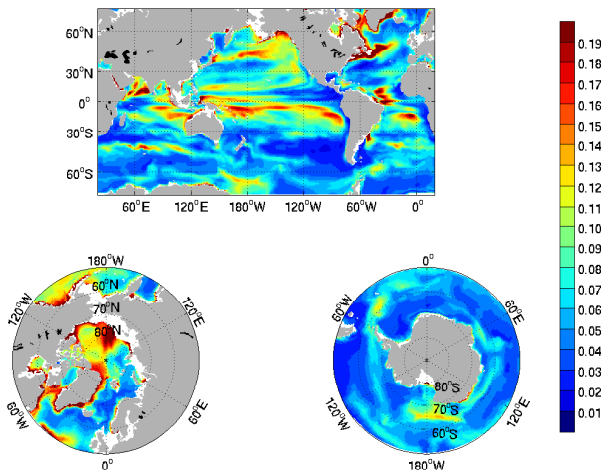
3D state variables

Figure: 1992-2011 standard deviation – salinity (in psu) at 105m

3D state variables

Figure: 1992-2011 mean – salinity (in psu) at 300m

3D state variables

Figure: 1992-2011 standard deviation – salinity (in psu) at 300m

3D state variables

Figure: 1992-2011 mean – salinity (in psu) at 910m

3D state variables

Figure: 1992-2011 standard deviation – salinity (in psu) at 910m
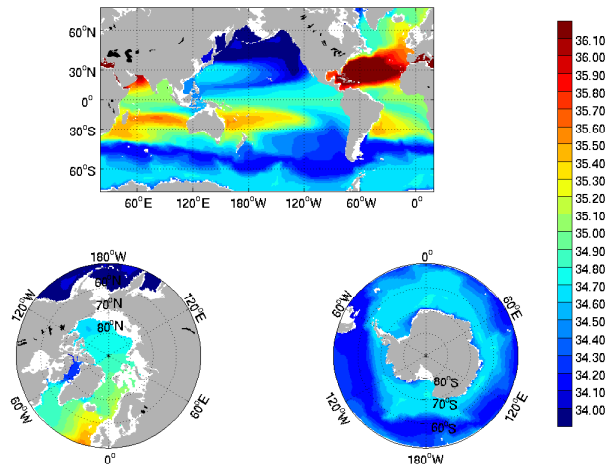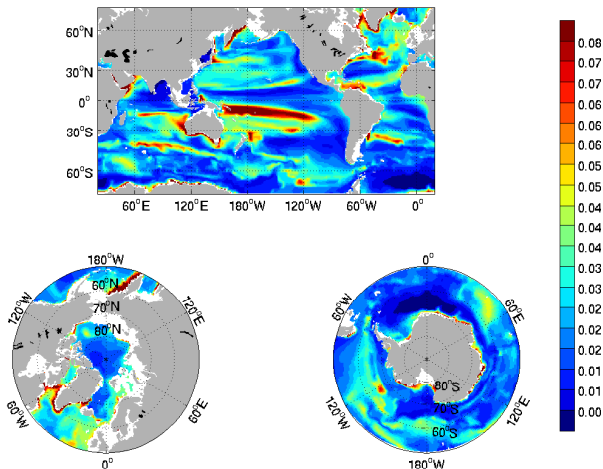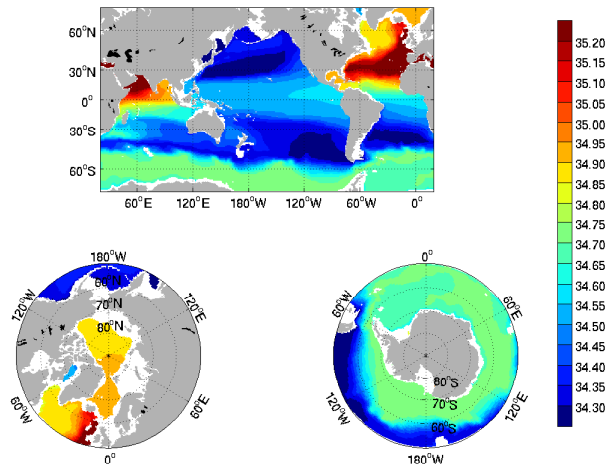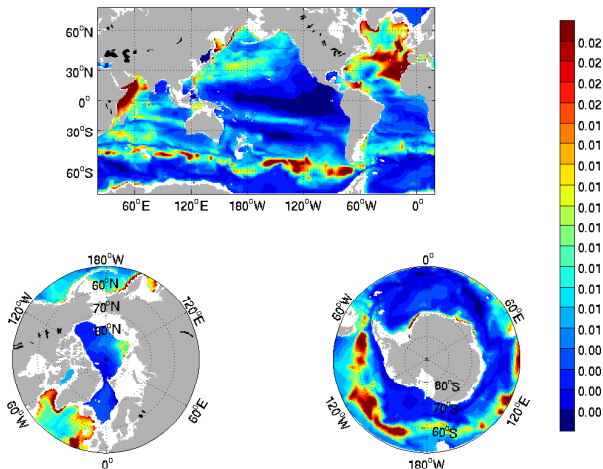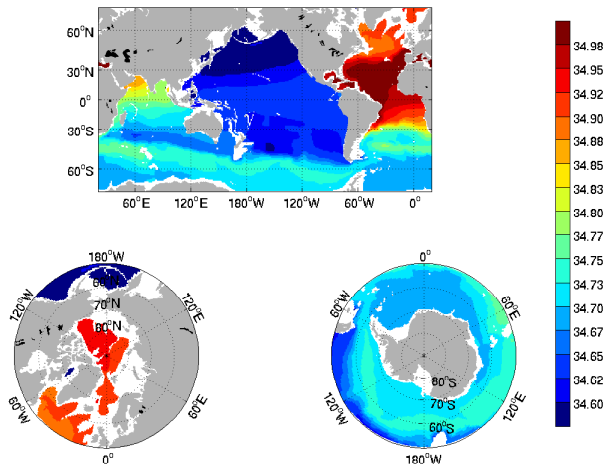
3D state variables

Figure: 1992-2011 mean – salinity (in psu) at 1914m
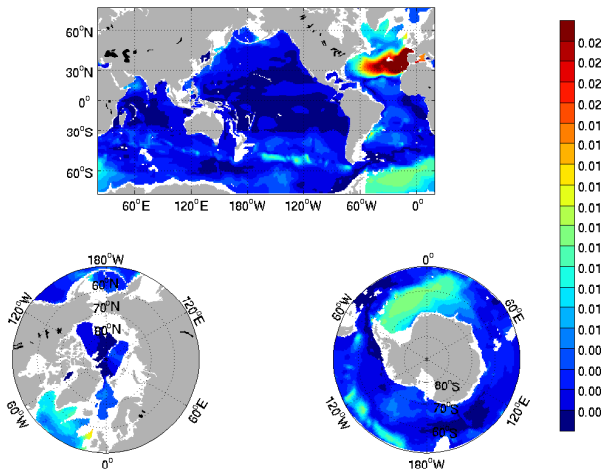
3D state variables

Figure: 1992-2011 standard deviation – salinity (in psu) at 1914m
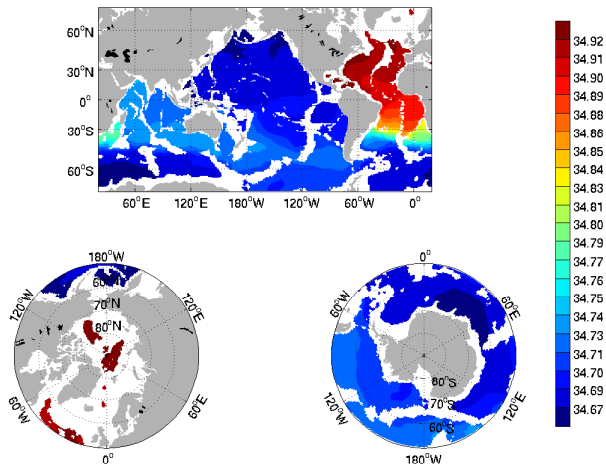
3D state variables

Figure: 1992-2011 mean – salinity (in psu) at 3581m
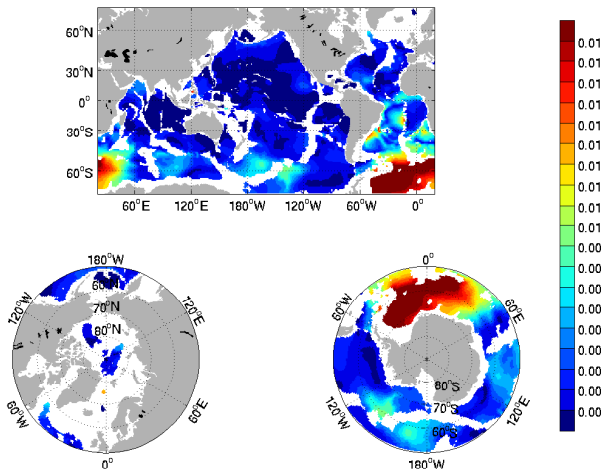
3D state variables

Figure: 1992-2011 standard deviation – salinity (in psu) at 3581m

3D state variables

Figure: 1992-2011 mean – vertical velocity (in mm/year) at 15m

3D state variables

Figure: 1992-2011 standard deviation – vertical velocity (in mm/year) at 15m
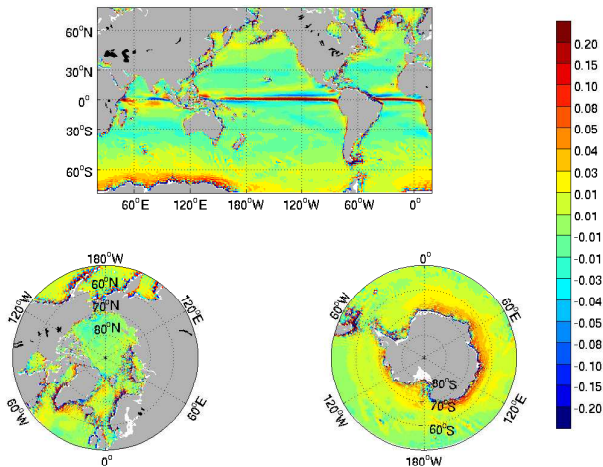
3D state variables

Figure: 1992-2011 mean – vertical velocity (in mm/year) at 105m
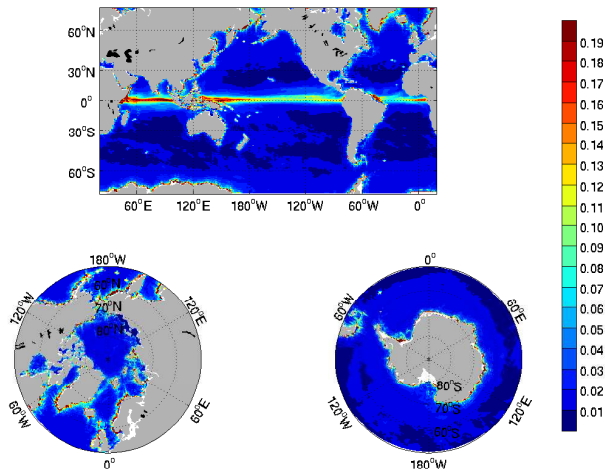
3D state variables

Figure: 1992-2011 standard deviation – vertical velocity (in mm/year) at 105m

3D state variables

Figure: 1992-2011 mean – vertical velocity (in mm/year) at 300m

3D state variables

Figure: 1992-2011 standard deviation – vertical velocity (in mm/year) at 300m
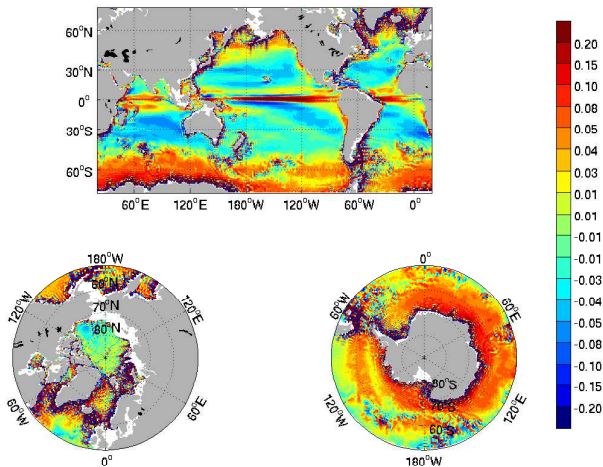
3D state variables

Figure: 1992-2011 mean – vertical velocity (in mm/year) at 910m
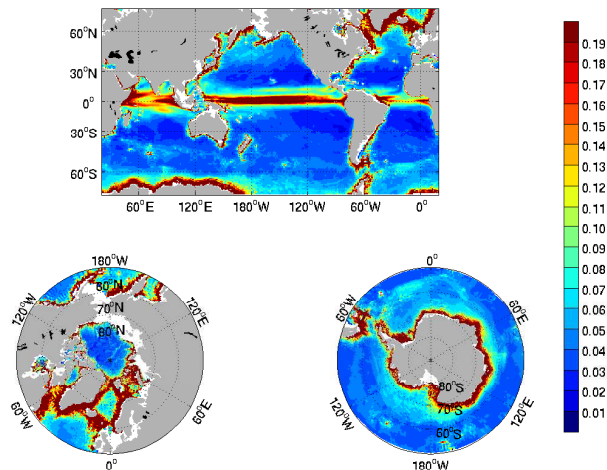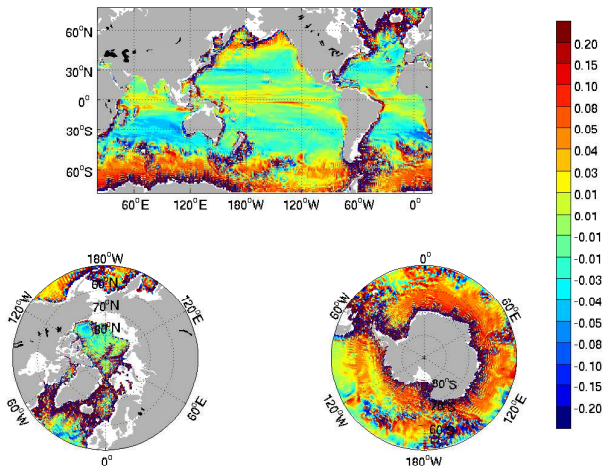
3D state variables

Figure: 1992-2011 standard deviation – vertical velocity (in mm/year) at 910m

3D state variables

Figure: 1992-2011 mean – vertical velocity (in mm/year) at 1914m

3D state variables
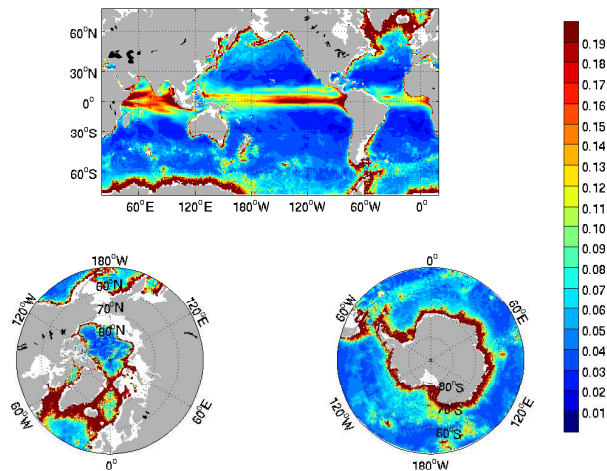

Figure: 1992-2011 standard deviation – vertical velocity (in mm/year) at 1914m

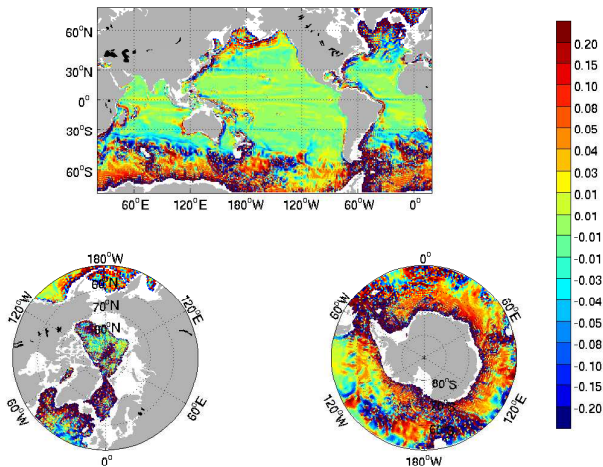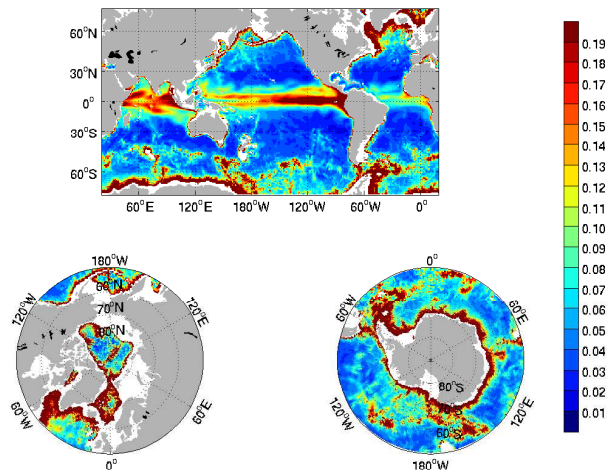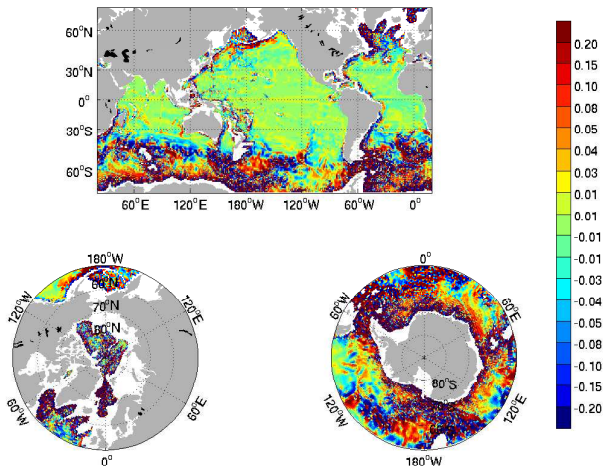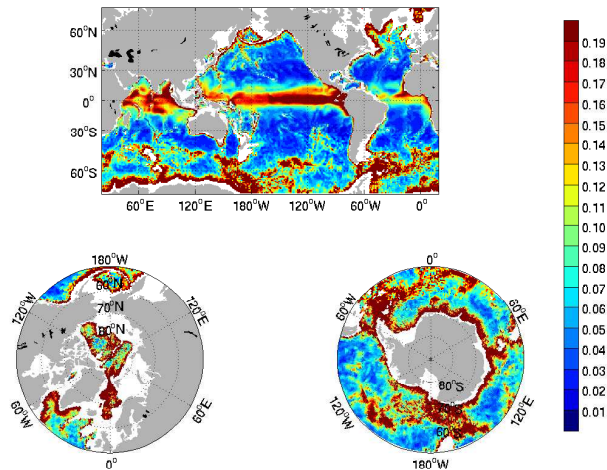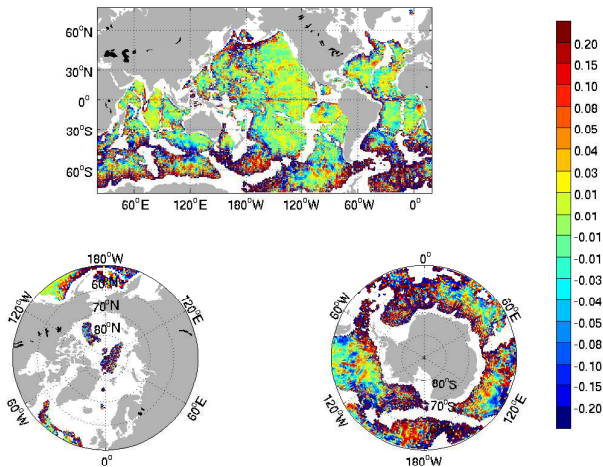# 3D state variables

Figure: 1992-2011 mean – vertical velocity (in mm/year) at 3581m
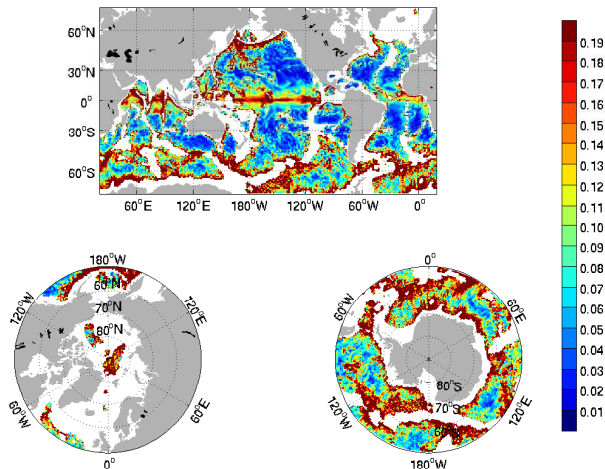
3D state variables

Figure: 1992-2011 standard deviation – vertical velocity (in mm/year) at 3581m
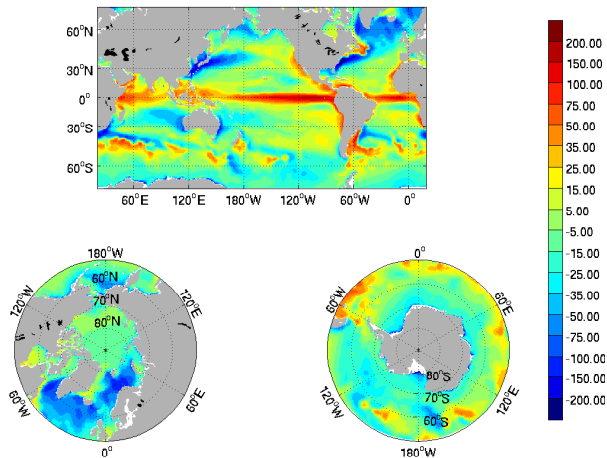
air-sea heat flux

Figure: 1992-2011 mean – QNET to ocean+ice (W/m^2)
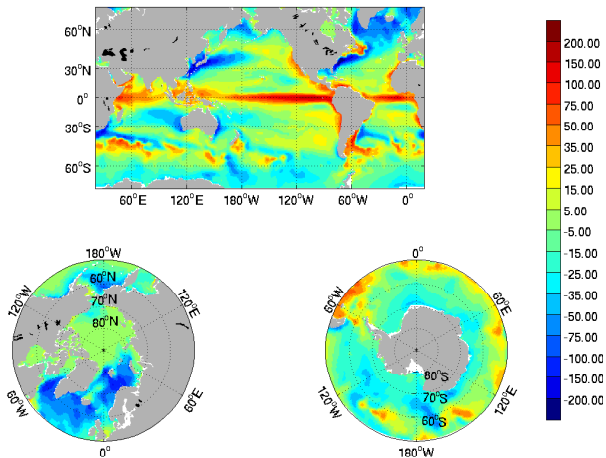
air-sea heat flux

Figure: 1992-2011 mean – QNET to ocean (W/m^2)
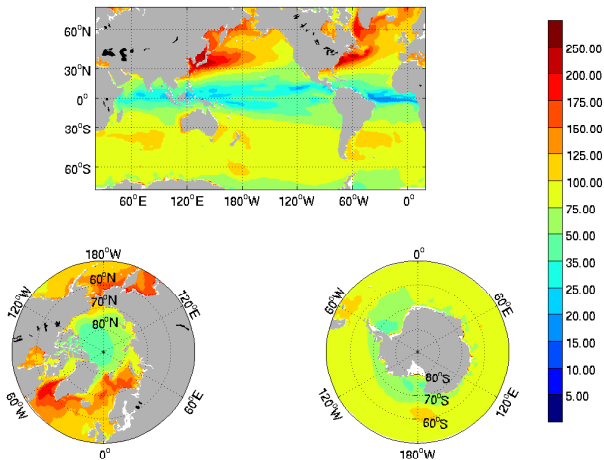
air-sea heat flux

Figure: 1992-2011 standard deviation – QNET to ocean+ice
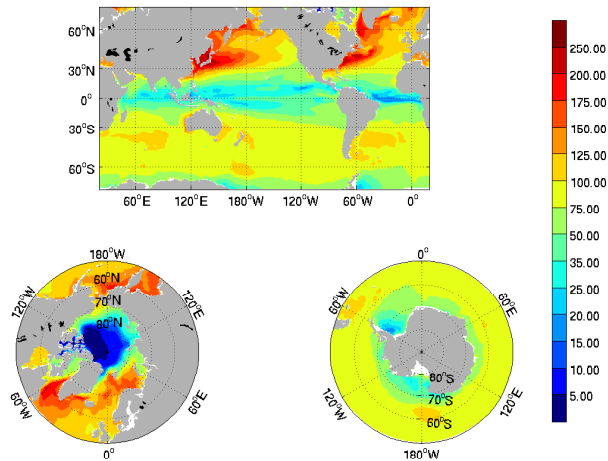(W/m^2)

air-sea heat flux

Figure: 1992-2011 standard deviation – QNET to ocean (W/m^2)
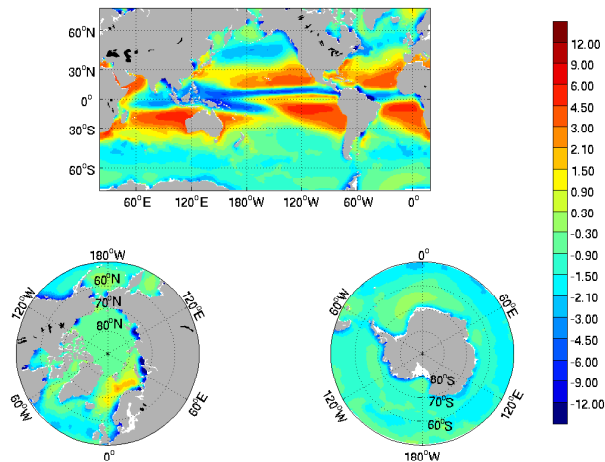
air-sea freshwater flux

Figure: 1992-2011 mean – E-P-R from ocean+ice (mm/day)
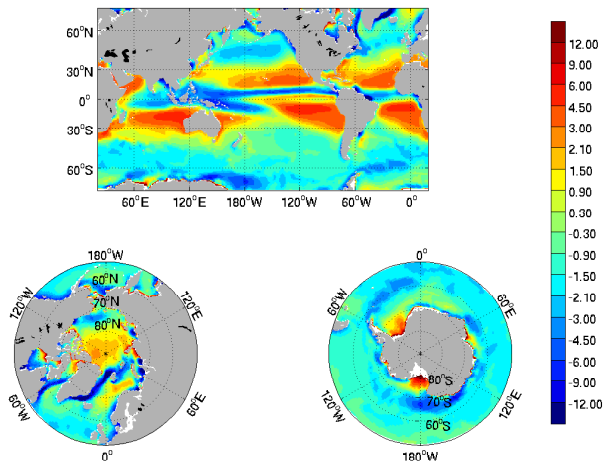
air-sea freshwater flux

Figure: 1992-2011 mean – E-P-R from ocean (mm/day)

air-sea freshwater flux

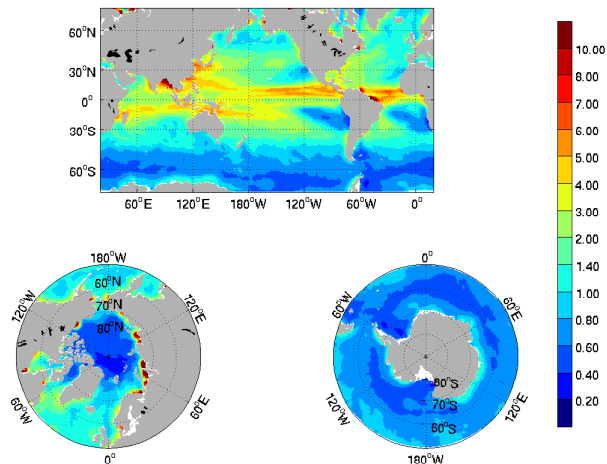Figure: 1992-2011 standard deviation – E-P-R to ocean+ice
(W/m^2)

air-sea freshwater flux
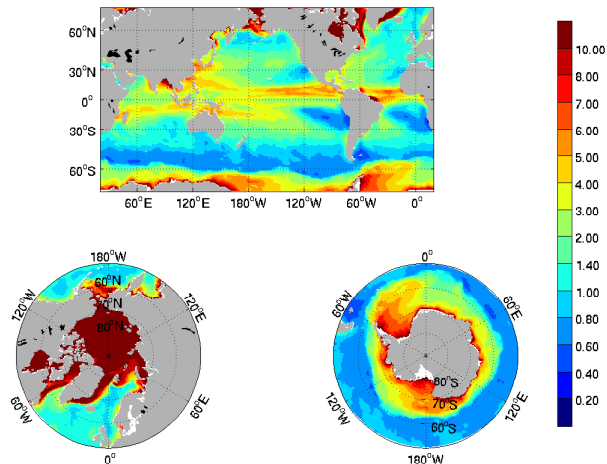

Figure: 1992-2011 standard deviation – E-P-R to ocean (W/m^2)
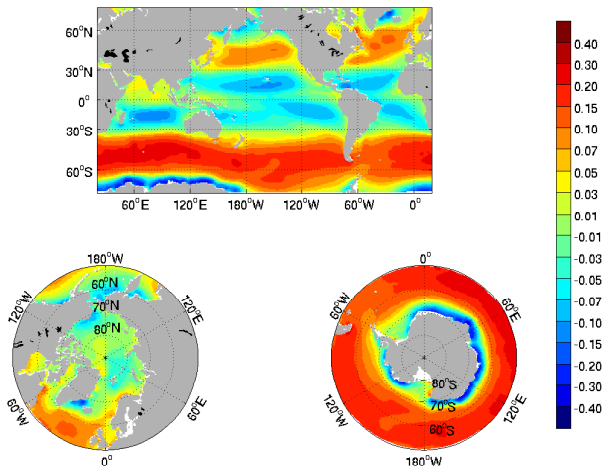
surface wind stress

Figure: 1992-2011 mean – zonal wind stress (N/m^2)
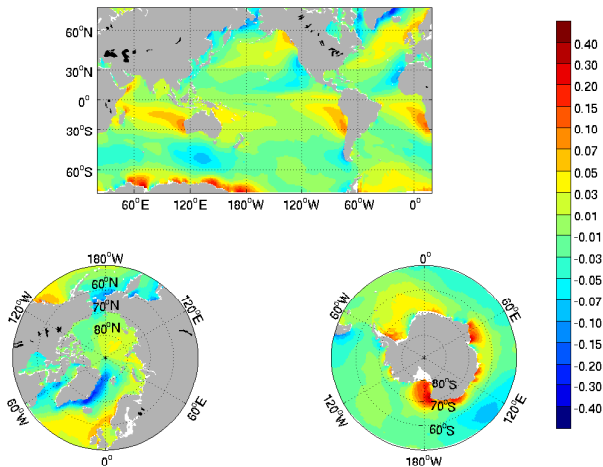
surface wind stress

Figure: 1992-2011 mean – meridional wind stress (N/m^2)

surface wind stress
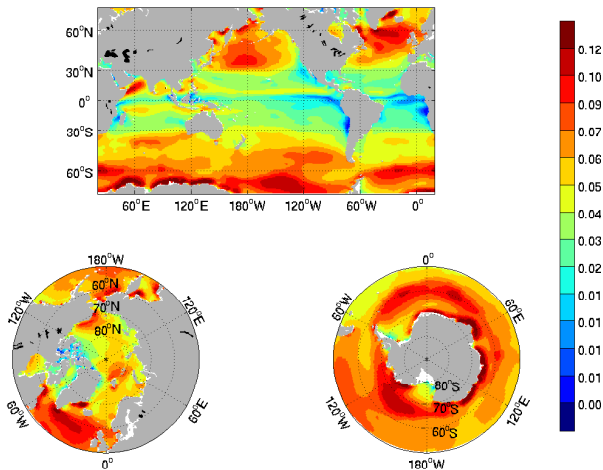

Figure: 1992-2011 standard deviation – tauZ (W/m^2)

surface wind stress
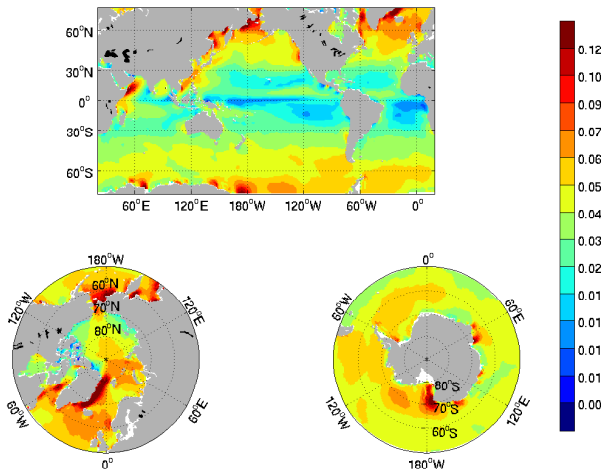

Figure: 1992-2011 standard deviation – tauM (W/m^2)

zonal mean tendencies

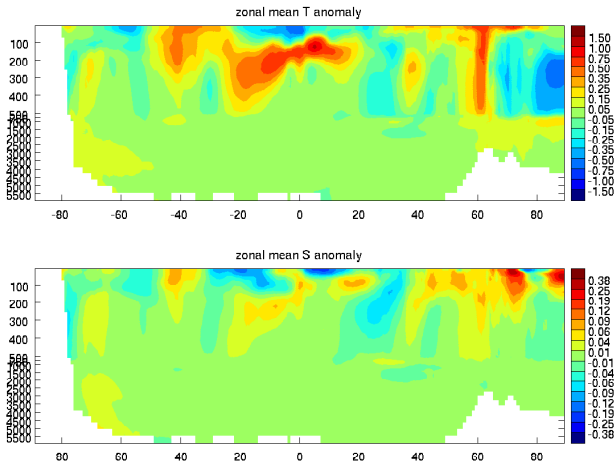Figure: 1992-2011 , last year minus first year – zonal mean temperature (degC; top) and salinity (psu; bottom)

equatorial sections

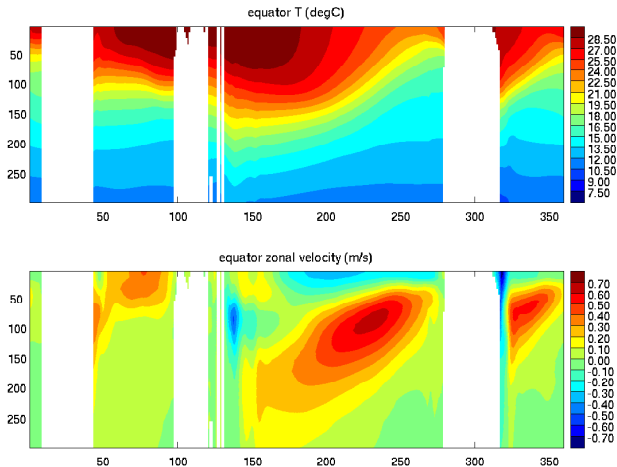Figure: 1992-2011 mean – equator temperature (degC;top) and zonal velocity (m/s;bottom)

global mean properties

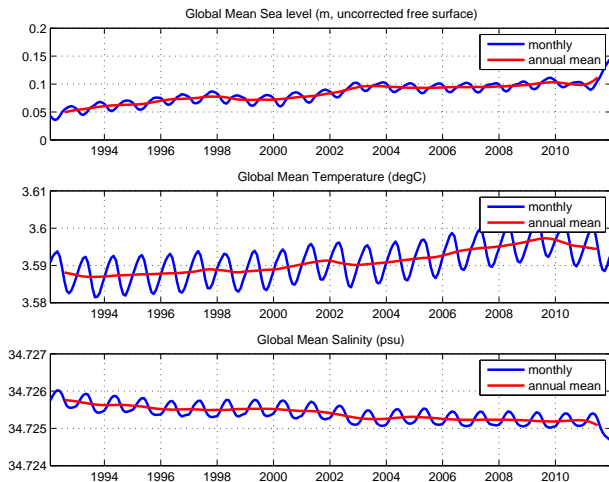Figure: global mean T (degC; top) and S (psu; bottom)

global mean properties

Figure: global mean temperature (K; top) and salinity (psu; bottom) minus first year

zonal mean properties

Figure: mean temperature (top; K) and salinity (bottom; psu) minus first year at lat ≈ -75

zonal mean properties

Figure: mean temperature (top; K) and salinity (bottom; psu) minus first year at lat ≈ -65

zonal mean properties

Figure: mean temperature (top; K) and salinity (bottom; psu) minus first year at lat ≈ -45
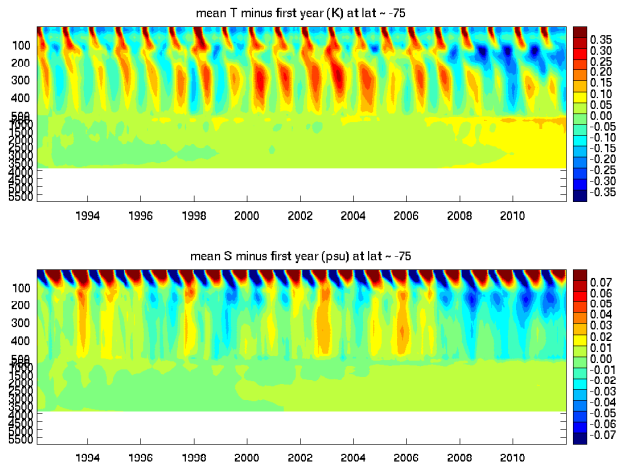
zonal mean properties

Figure: mean temperature (top; K) and salinity (bottom; psu) minus first year at lat ≈ -25

zonal mean properties

Figure: mean temperature (top; K) and salinity (bottom; psu) minus first year at lat ≈ 0

zonal mean properties

Figure: mean temperature (top; K) and salinity (bottom; psu) minus first year at lat ≈ 25
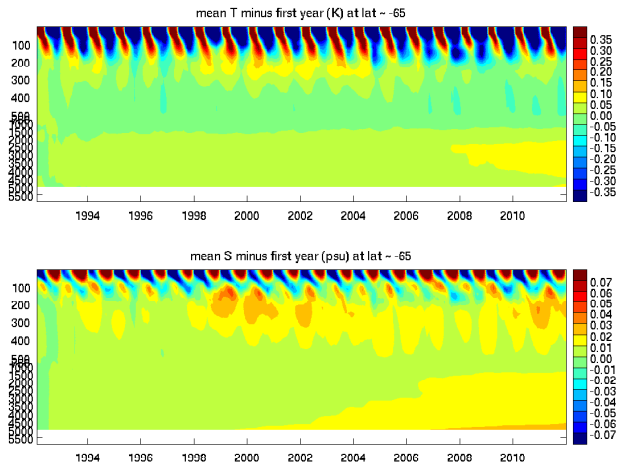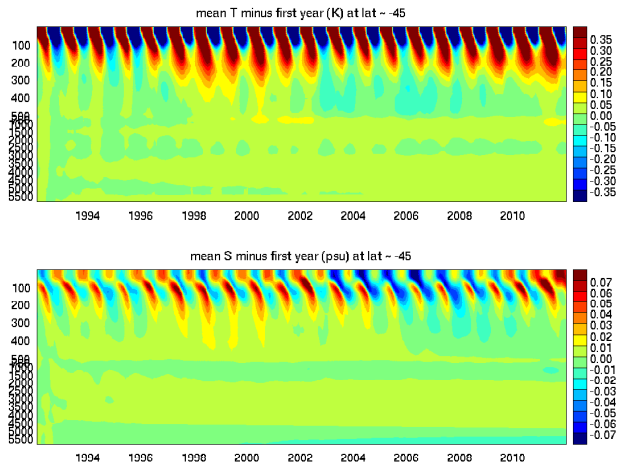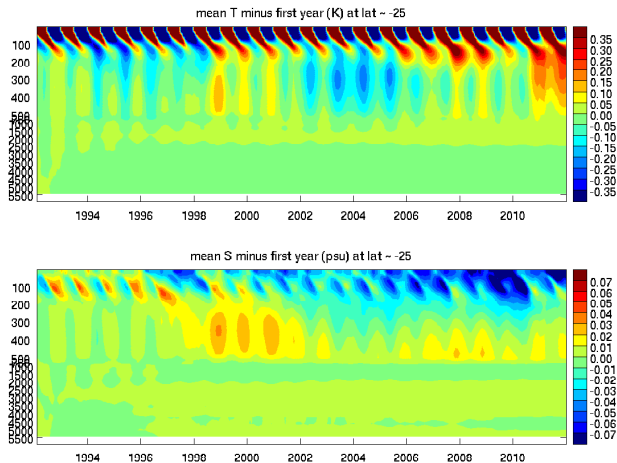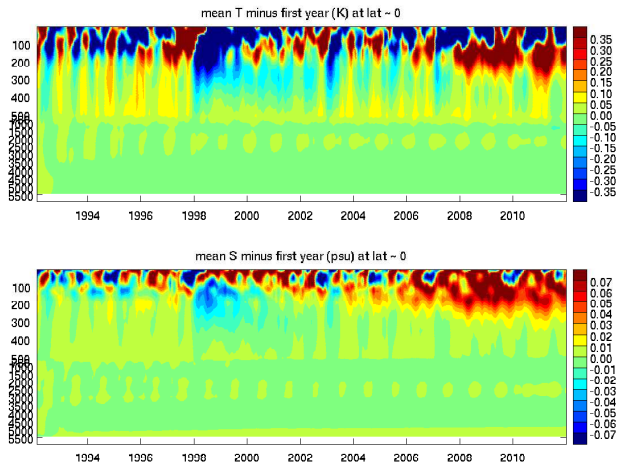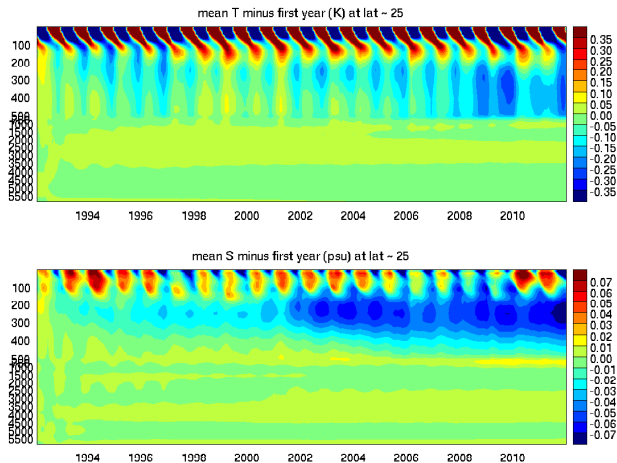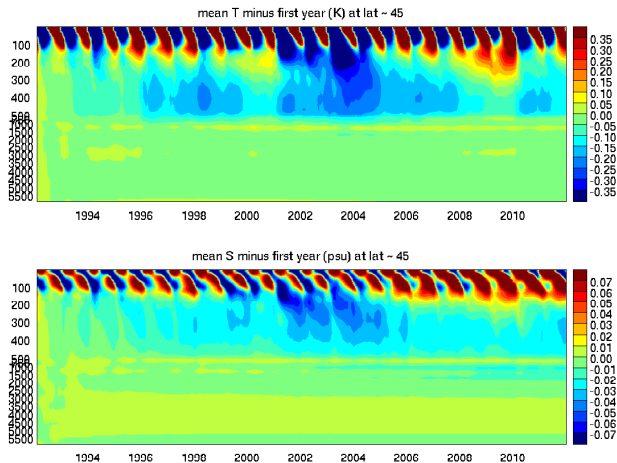
zonal mean properties

Figure: mean temperature (top; K) and salinity (bottom; psu) minus first year at lat ≈ 45

zonal mean properties

Figure: mean temperature (top; K) and salinity (bottom; psu) minus first year at lat $\approx$ 65

zonal mean properties

Figure: mean temperature (top; K) and salinity (bottom; psu) minus first year at lat ≈ 75
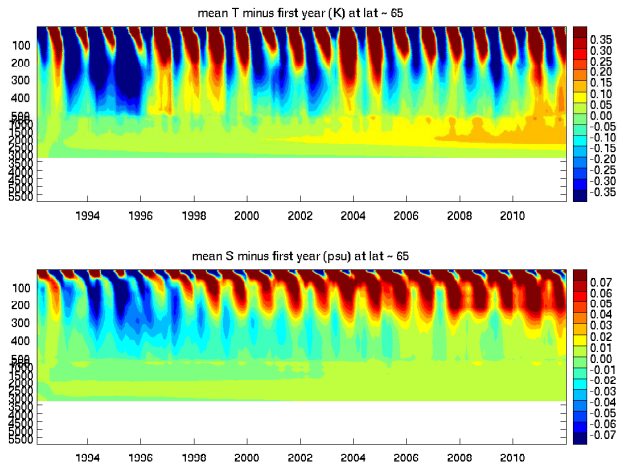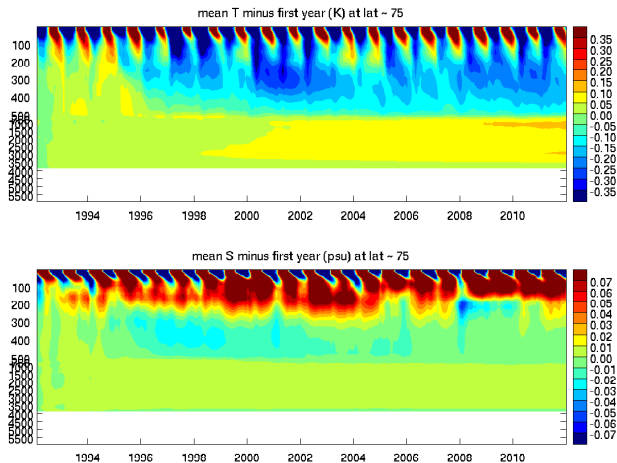
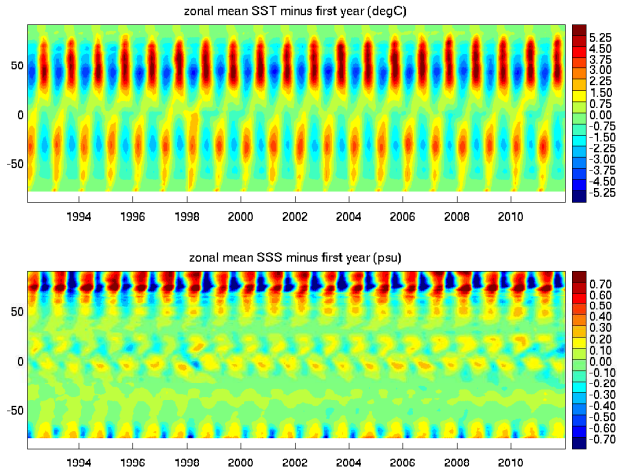# zonal mean properties (surface)

Figure: zonal mean temperature (degC; top) and salinity (psu; bottom) minus first year (psu) at 5m depth
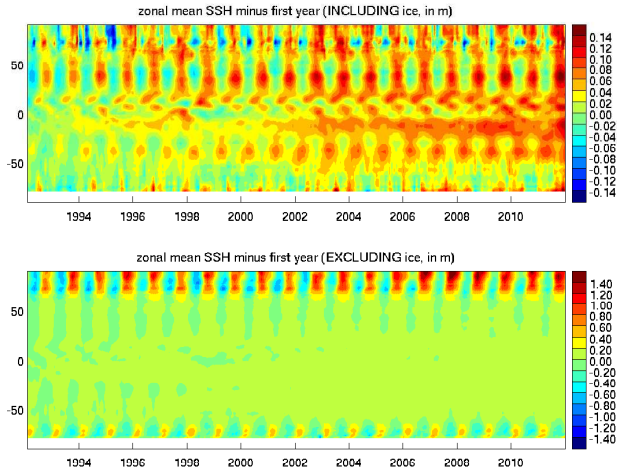
zonal mean properties (surface)

Figure: zonal mean SSH (m, uncorrected free surface) minus first year, including ice (top) and below ice (bottom)

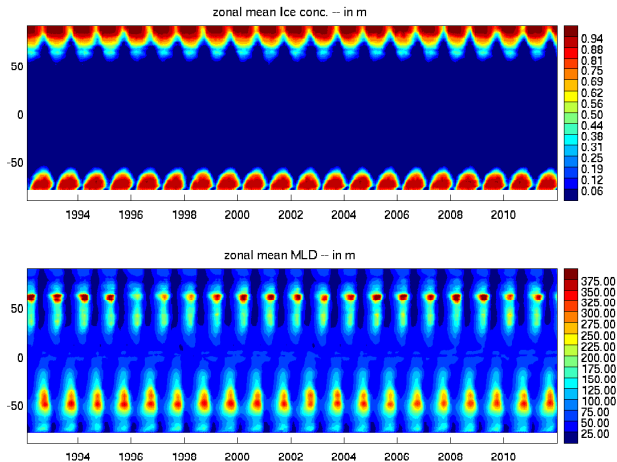# zonal mean properties (surface)

Figure: zonal mean ice concentration (no units) and mixed layer depth (m)
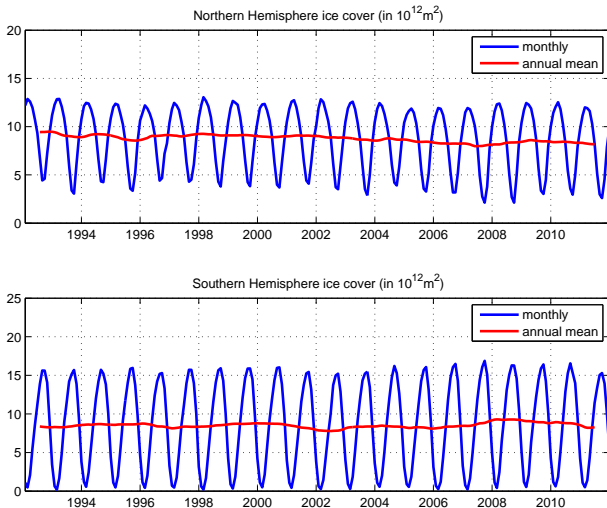
seaice time series

Figure: sea ice cover (in $10^{12} m^2$) in northern (top) and southern (bottom) hemisphere
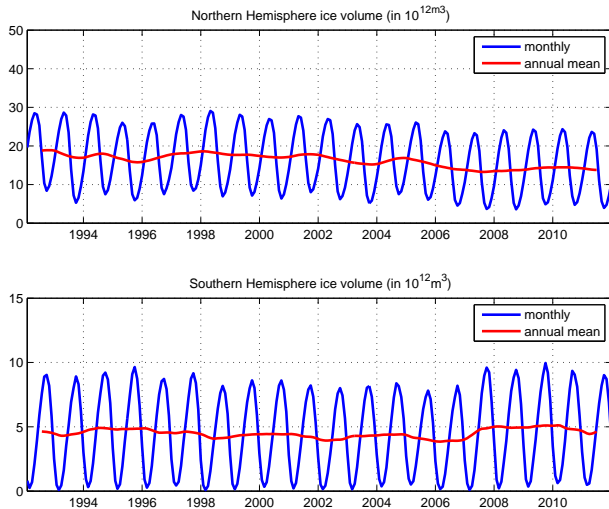
seaice time series

Figure: sea ice volume (in $10^{12} m^3$) in northern (top) and southern (bottom) hemisphere
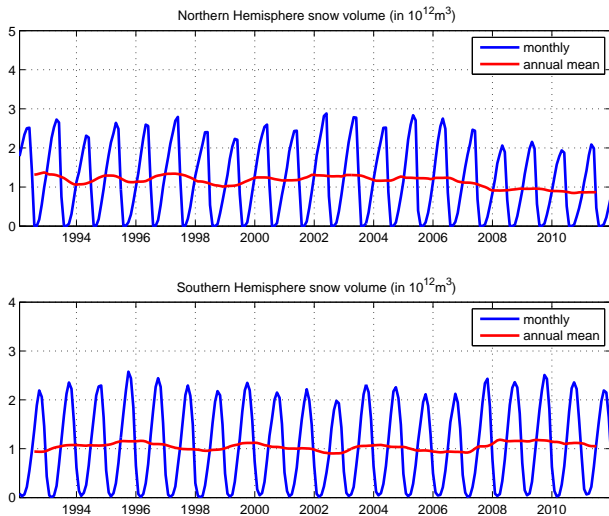
seaice time series

Figure: snow volume (in $10^{12} m^3$) in northern (top) and southern (bottom) hemisphere
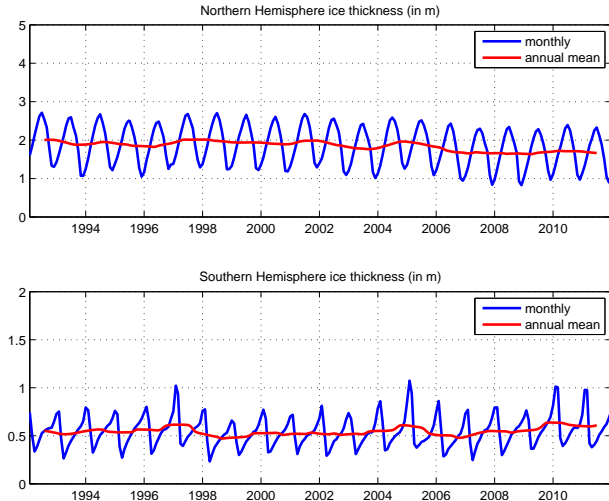
seaice time series

Figure: sea ice thickness (in m) in northern (top) and southern (bottom) hemisphere
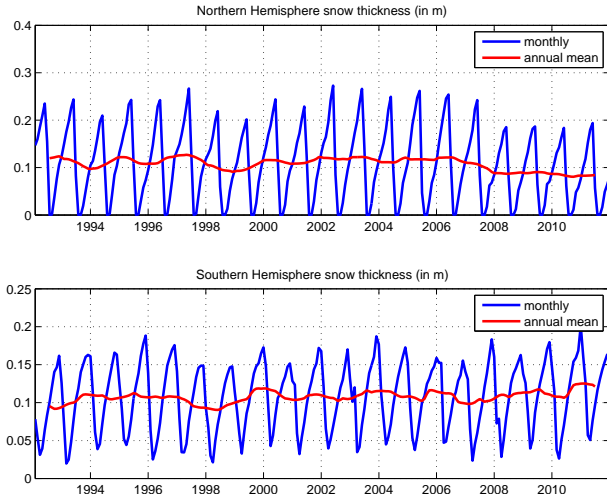
seaice time series

Figure: snow thickness (in m) in northern (top) and southern (bottom) hemisphere

budgets : volume, heat and salt (top to bottom)

Figure: 1992-2011 global (upper) north (mid) and south (lower), mass budget (ocean+ice) in kg/m^2.

budgets : volume, heat and salt (top to bottom)

Figure: 1992-2011 global (upper) north (mid) and south (lower), mass budget (ice only) in kg/m^2.

budgets : volume, heat and salt (top to bottom)

Figure: 1992-2011 global (upper) north (mid) and south (lower), mass budget (ocean only) in kg/m^2.

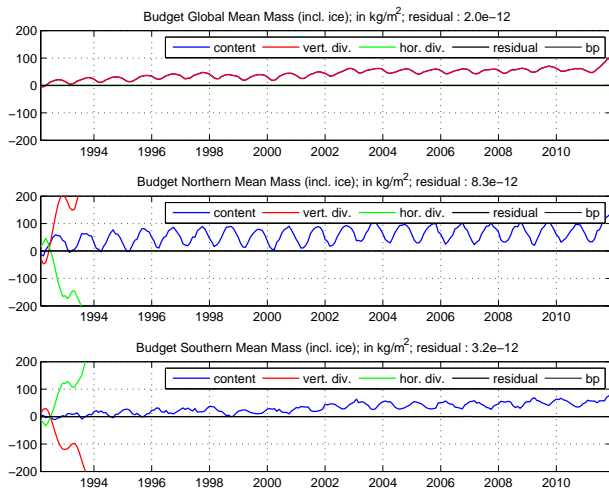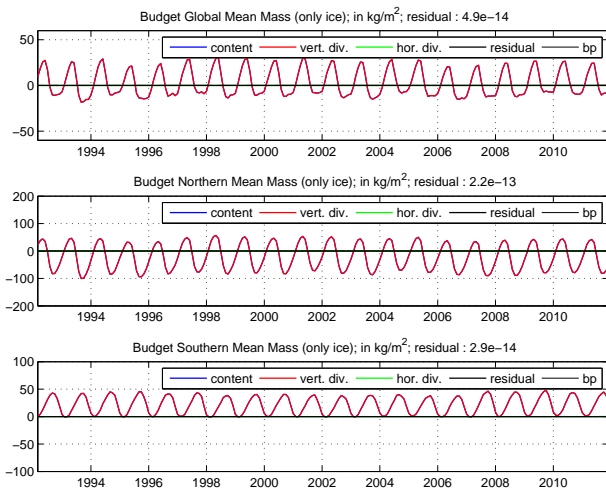# budgets : volume, heat and salt (top to bottom)

Figure: 1992-2011 global (upper) north (mid) and south (lower), heat budget (ocean+ice) in J/m^2.

budgets : volume, heat and salt (top to bottom)

Figure: 1992-2011 global (upper) north (mid) and south (lower), heat budget (ice only) in J/m^2.

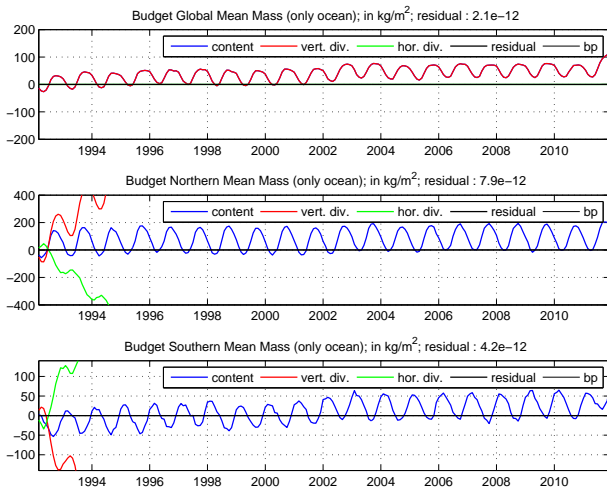# budgets : volume, heat and salt (top to bottom)

Figure: 1992-2011 global (upper) north (mid) and south (lower), heat budget (ocean only) in J/m^2.

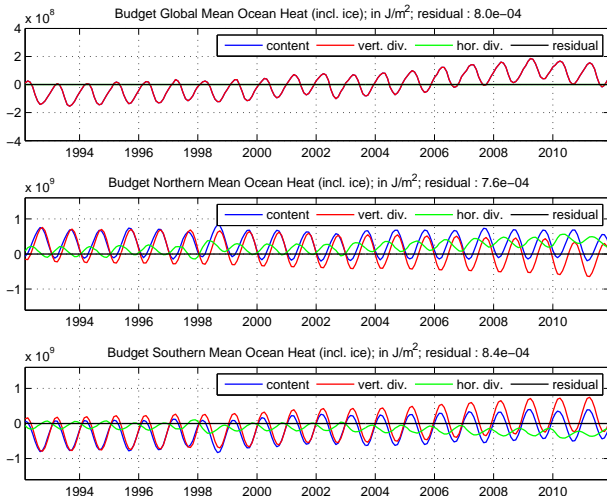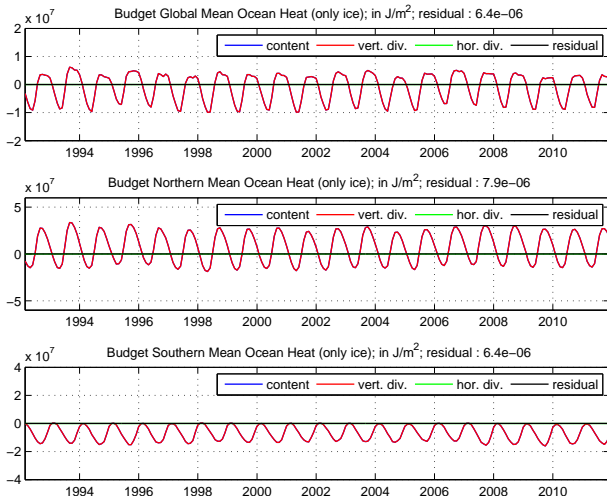# budgets : volume, heat and salt (top to bottom)

Figure: 1992-2011 global (upper) north (mid) and south (lower), salt budget (ocean+ice) in g/m^2.

budgets : volume, heat and salt (top to bottom)

Figure: 1992-2011 global (upper) north (mid) and south (lower), salt budget (ice only) in g/m².

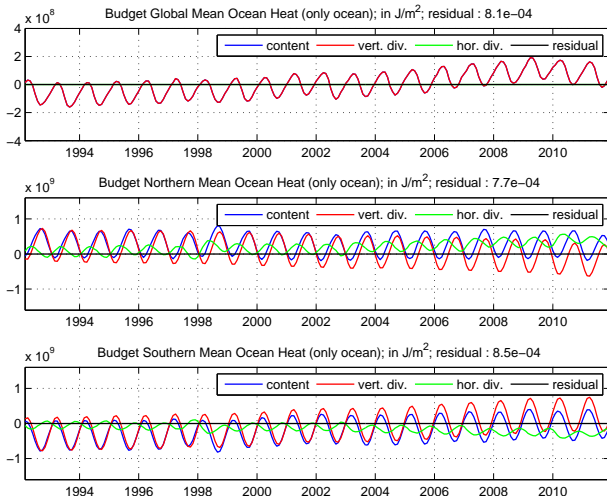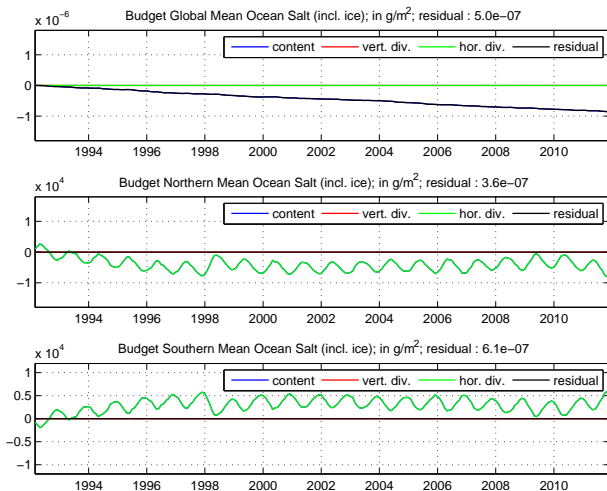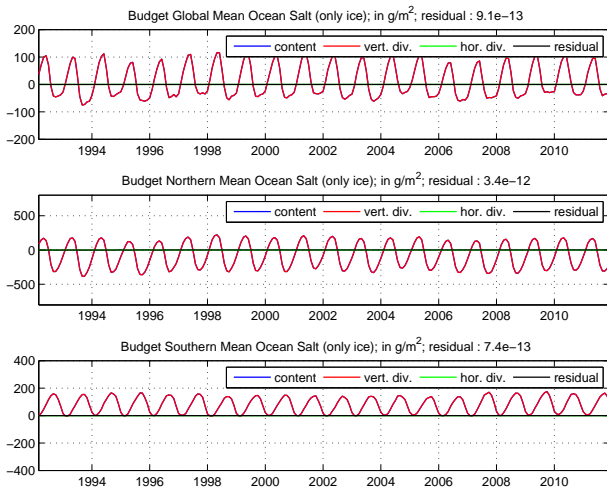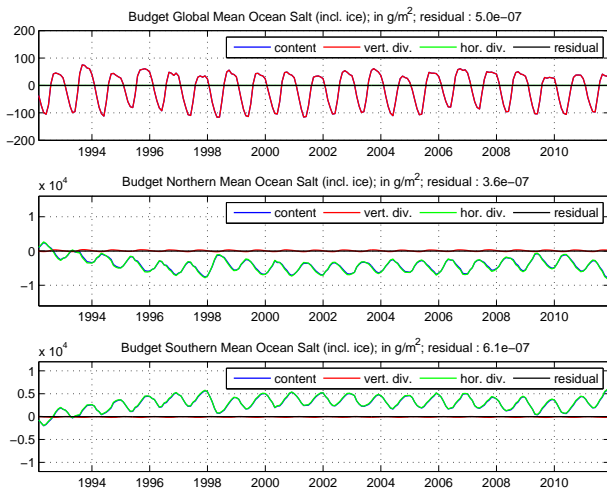# budgets : volume, heat and salt (top to bottom)

Figure: 1992-2011 global (upper) north (mid) and south (lower), salt budget (ocean only) in g/m^2.

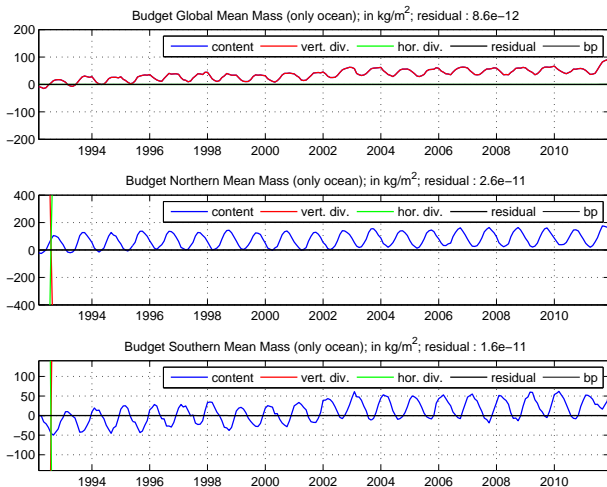# budgets : volume, heat and salt (100m to bottom)

Figure: 1992-2011 global (upper) north (mid) and south (lower), mass budget (ocean only) in kg/m².

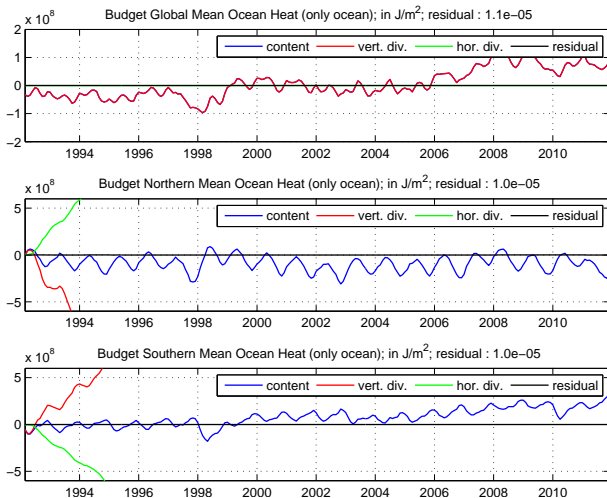# budgets : volume, heat and salt (100m to bottom)

Figure: 1992-2011 global (upper) north (mid) and south (lower), heat budget (ocean only) in J/m^2.

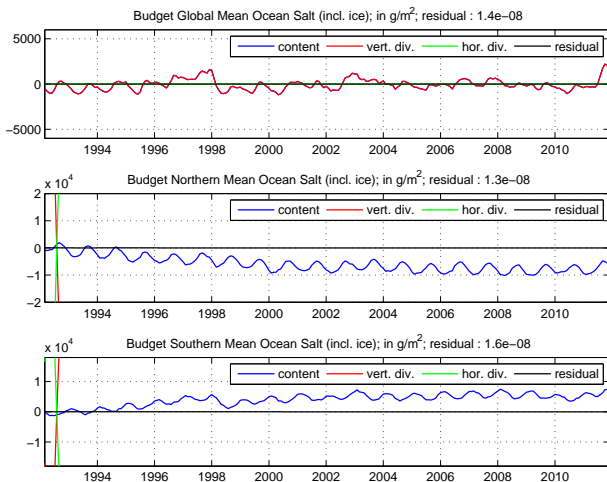# budgets : volume, heat and salt (100m to bottom)

Figure: 1992-2011 global (upper) north (mid) and south (lower), salt budget (ocean only) in g/m^2.
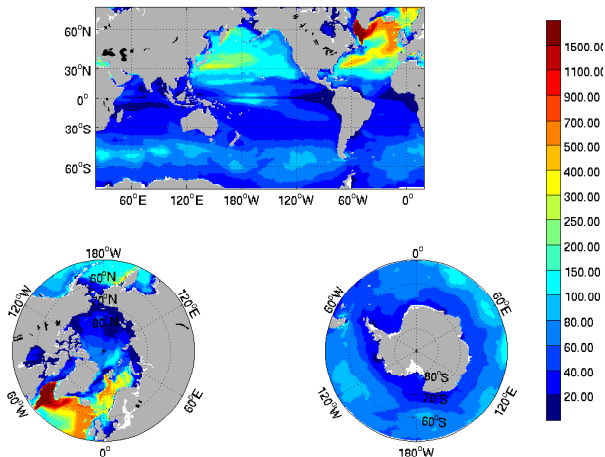
mixed layer depth fields

Figure: 1992-2011 March mean – mixed layer depth per Kara formula (m)
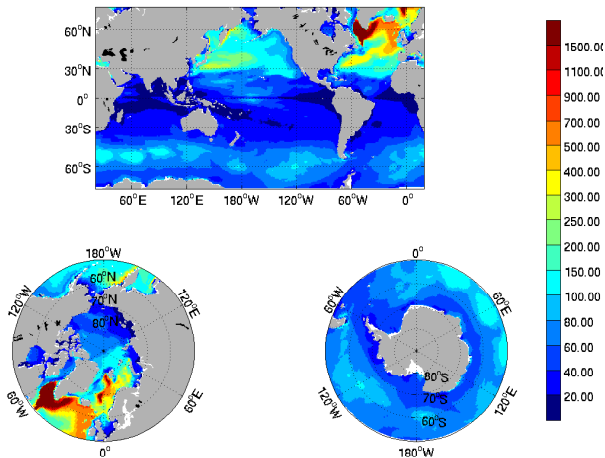
mixed layer depth fields

Figure: 1992-2011 March mean – mixed layer depth per Suga formula (m)
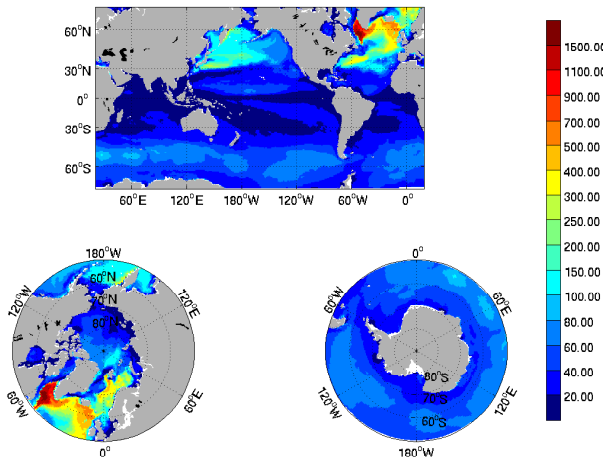
mixed layer depth fields

Figure: 1992-2011 March mean – mixed layer depth per Boyer M. formula (m)
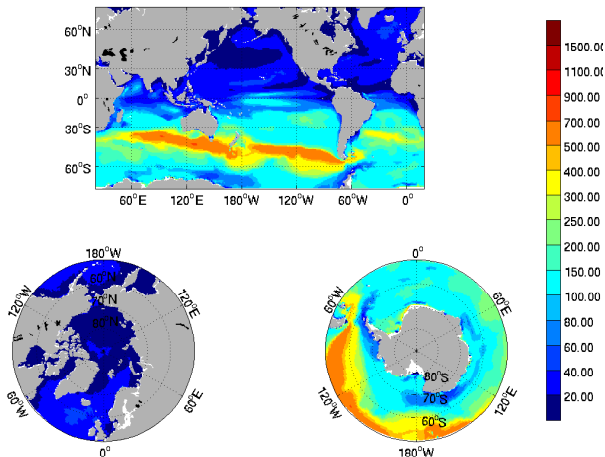
mixed layer depth fields

Figure: 1992-2011 September mean – mixed layer depth per Kara formula (m)
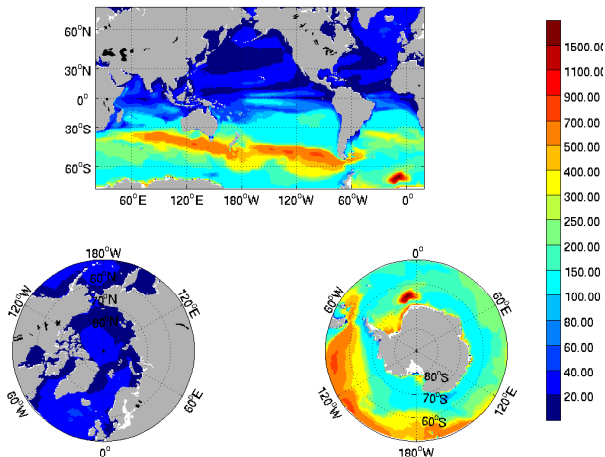
mixed layer depth fields

Figure: 1992-2011 September mean – mixed layer depth per Suga formula (m)
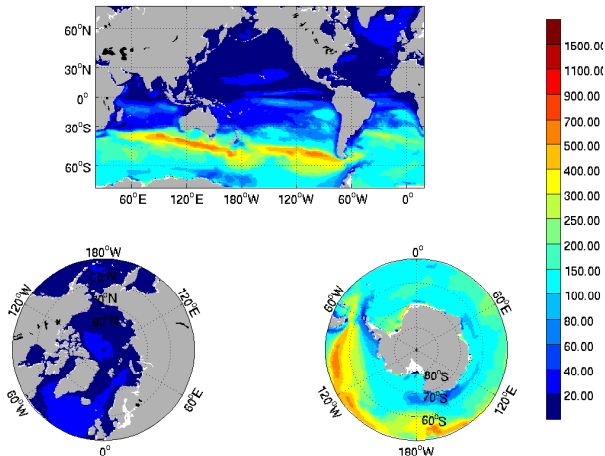
mixed layer depth fields

Figure: 1992-2011 September mean – mixed layer depth per Boyer M. formula (m)